Automated Robotic Assembly Using a Vibratory Work Table: Optimal Tuning of Vibrators Based on the Taguchi Method

by

Shih-Hung Li

S.B., Mechanical Engineering (1990)

University of Texas at Austin

Submitted to the Department of Mechanical Engineering

in Partial Fulfillment of the Requirements for the degree of

Master of Science in Mechanical Engineering

at the

Massachusetts Institute of Technology

January, 1992

Signature of Author _____

Department of Mechanical Engineering
January 17, 1992

Certified by _____

Dr. Haruhiko Asada
Professor
Thesis Supervisor

Accepted by _____

Dr. Ain A. Sonin
Chairman, Department Committee on Graduate Students

Automated Robotic Assembly Using a Vibratory Work Table:

Optimal Tuning of Vibrators Based on the Taguchi Method

by

Shih-Hung Li

S.B., University of Texas at Austin (1990)

Submitted to the Department of Mechanical Engineering on January 17th, 1992 in partial fulfillment of the requirements for the Degree of Master of Science in Mechanical Engineering

Abstract

The goal of this paper is to perform complex assembly tasks, using a robot assisted by a multi-axis vibrator that reduces friction and avoids jamming. An experiment-based approach using the Taguchi Method is applied to the tuning of the vibrator. The vibrators are tuned so that effects of friction and stick-slip can be minimized. Using actual assembly data and an experimental analysis method, called Taguchi analysis, we obtain optimal settings for the vibrator through an iterative procedure. The use of Taguchi Method is a new learning technique. The Taguchi Method has brought the true meaning of automation to reality by eliminating human intervention in operating the control console. A minimum number of tests or experiments are designed and conducted at each iteration, and the process is repeated until final results reach a satisfactory level. To evaluate performance, we use the root mean square of reaction force and moment during assembly, which indicates the magnitude of stick-slip and the effect of friction. The basic technique, a prototype system, and experimental results are presented in this paper. After we have proven the concept of using Taguchi Method as a new learning method, we then apply it to two dimensional cable connector assembly. The experimental setup and results are also presented.

Thesis Supervisor:

Haruhiko Asada
Professor
Mechanical Engineering, MIT

List of Figures

Automated Robotic Assembly Using a Vibratory Work Table:

Optimal Tuning of Vibrators Based on the Taguchi Method

by

Shih-Hung Li

S.B., University of Texas at Austin (1990)

Submitted to the Department of Mechanical Engineering on January 17th, 1992 in partial fulfillment of the requirements for the Degree of Master of Science in Mechanical Engineering

Abstract

The goal of this paper is to perform complex assembly tasks, using a robot assisted by a multi-axis vibrator that reduces friction and avoids jamming. An experiment-based approach using the Taguchi Method is applied to the tuning of the vibrator. The vibrators are tuned so that effects of friction and stick-slip can be minimized. Using actual assembly data and an experimental analysis method, called Taguchi analysis, we obtain optimal settings for the vibrator through an iterative procedure. The use of Taguchi Method is a new learning technique. The Taguchi Method has brought the true meaning of automation to reality by eliminating human intervention in operating the control console. A minimum number of tests or experiments are designed and conducted at each iteration, and the process is repeated until final results reach a satisfactory level. To evaluate performance, we use the root mean square of reaction force and moment during assembly, which indicates the magnitude of stick-slip and the effect of friction. The basic technique, a prototype system, and experimental results are presented in this paper. After we have proven the concept of using Taguchi Method as a new learning method, we then apply it to two dimensional cable connector assembly. The experimental setup and results are also presented.

Thesis Supervisor:

Haruhiko Asada
Professor
Mechanical Engineering, MIT

To my parents

An idea is the only lever which really moves the world.

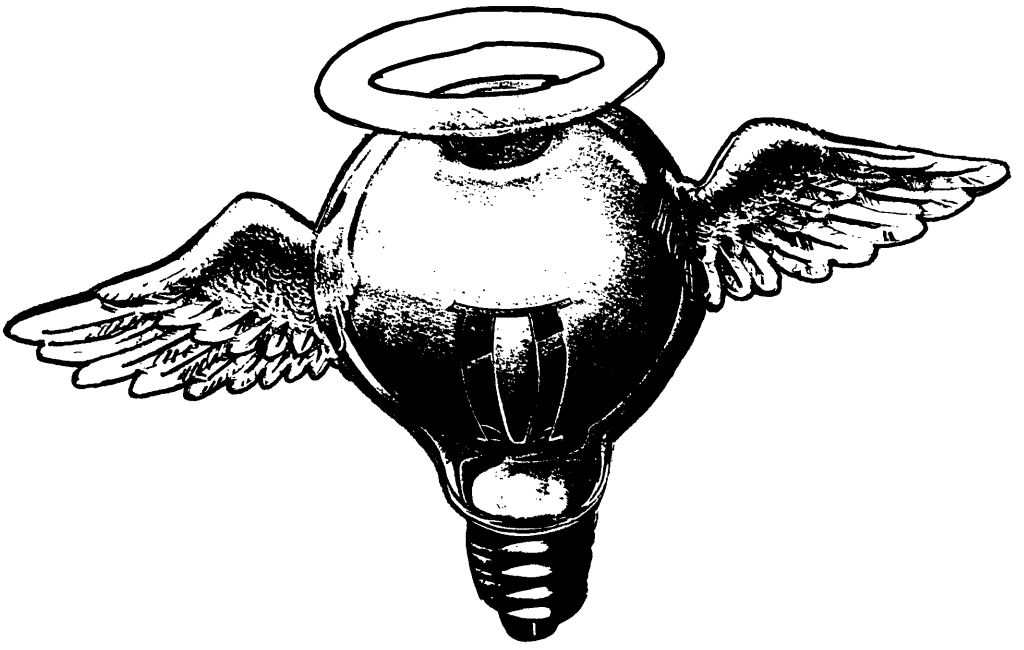

Some people entertain ideas, others put them to work.

Acknowledgement

I am most grateful to my parents who made a most crucial decision to send me abroad eight years ago. If not for that decision, I am sure that I would not be what I am now. I would like to thank them and my sister for the many sacrifices they have made for my sake, for giving me emotional and financial support, and most of all, for being there when I needed them.

I would also like to thank my godparents, my "sister", and "brothers" who have given me a home and family for the past eight years.

I would like to take this opportunity to thank Matsushita Electric Ltd. for supporting this project and to express my sincere gratitude to Mr. Kenji Okamoto for teaching me so much and helping me to understand the hardware in a such short time. I would also like to thank Mr. Noriaki Yoshida for his assistance.

I would like to express my deepest thanks and respect to Professor Haruhiko Asada, whose painstaking instruction and advice have helped me grow both academically and personally. His unique suggestions and ideas have inspired me to explore deeper in my studies instead of merely scratching on the surface.

I would also like to thank my colleagues in the Intelligent Machine Laboratory who have given me a great deal of advice and support and have certainly made my stay at the lab a wonderful experience. I would also like to thank the *Panasonic* robot who was kind enough to cooperate by functioning normally and the couch in my office which provided a temporary "home" for me after late nights at the lab.

I would also like to thank my roommates, Chen-an Chen and Ting-Jen Yeh for putting up with me for so long. There are so many people I must thank that it would be impossible to mention you all. I thank all the dear friends I made during my stay at MIT, for giving me the moral support I needed and for helping me in times of need.

Contents

Chapter 1
Introduction

The assembly of printed circuit boards (pc board) has been performed very efficiently by insertion machines. Those assembly machines are operated at high speed and low costs, but still have difficulty in dealing with odd-shaped components such as heat sinks, connectors, and other non-standard parts. Most of those "odd-shaped" components are still manually inserted into pc boards, which are a bottleneck of automation.

Assembly has been addressed by a number of research groups including [Simunovic, 1979], [Whitney, 1982], [Mason, 1982], [Lozano-Perez et al., 1984], and [Asada and Hirai, 1990], and [McCarragher and Asada 1991]. [Whitney, 1982] used Remote-Center-Compliance (RCC) hand to describe the use of passive compliance as an aid for the insertion process. [McCarragher and Adada 1991] treated the whole assembly process as a discrete dynamic process as compared to the quasi-static process proposed by [Whitney, 1982]. [Asada and Okamoto] used the neural-network with the back-propagation method to complete the assembly process. [Dupuis 1992] studied the assembly process by translating human-skills to the machine. These techniques are in general based on compliance and force sensing, which are effective for coping with geometric uncertainty and misalignment. However, difficulties dealing with greater uncertainties arise from to friction. Friction is highly nonlinear, and unpredictable. It disturbs force sensing and smooth operations. The problem becomes harder when we deal with complex, odd-shaped parts; they often have burrs and unfinished surfaces, which prevent smooth insertion operation and cause jamming.

The goal of this research is to develop a technique for complex robotic assembly using a passive compliance and active vibration worktable. The vibratory assembly table assists the robot by generating dither that breaks down equilibrium force conditions between the contact forces and robotic applied forces, thus allowing the workpiece to move smoothly. Our target task is to develop an effective way to tune the vibrator in order to virtually reduce friction and stick-slip. Parameters for controlling the vibrator, eg. frequencies, amplitudes, and phases, are optimized by using an experimental robust optimization technique.

In Chapter 2, we will describe the assembly task discussed in this paper. Chapter 3 discusses the reason why the Taguchi Method is implemented and will include a brief overview of the Taguchi Method. A more detailed description of this robust optimization technique, also known as the Robust Design, is given in Appendix C[Phadke, 1989]. In Chapter 4, we will explain how we evaluate the assembly operation qualitatively and how we actually minimize the performance index. 1-D concept proving experimental data are also presented in Chapter 4 to support our approach. Chapter 5 presents 2-D cable insertion test results. Finally, Chapter 6 presents the conclusion and future development of this method.

Chapter 2

The Problem and Approach

2.1 Friction and Stick-Slip in Assembly

Assembly is the process of mating a geometrically constrained workpiece with its environment. Most of the odd-shaped electronic parts such as heat sinks and connectors are made by molding, forming, drawing, or cutting sheet metals and composites. These manufacturing processes result in rough surfaces and edges around the parts. As those parts slide across printed circuit boards during assembly operations, they encounter large frictional forces. These frictional forces often cause unwanted motion such as stick-slip and jamming. In the worst case, the mating workpiece may be permanently damaged or get stuck in the machine. The damaged part halts the assembly line, which results in an increase of manufacturing costs. Our main task here is to reduce the chance of stick-slip and jamming. Therefore, we need to understand the physical behavior of frictional contacts and develop a method for quantifying the behavior.

Friction significantly affects performance of almost all the servo-controlled machines. Friction becomes a dominating factor especially for precise motions at low velocities. Friction determines the range of displacements and velocities at which the mechanism can operate. The minimum achievable displacement and sustainable velocity arise from a periodic process of sticking and sliding, a motion called stick-slip. The stick-slip was first studied by [Thomas 1930] using the static plus kinetic friction model shown in Figure G.1. [Bowden and Leben 1939] demonstrated that

sticking occurs and coined the term stick-slip. However, it has been proven through macroscopic observation that the static plus kinetic friction model is inadequate to explain the observed phenomena. [Sampson *et al.* 1943] [Dokos 1943] [Rabinowicz 1951] used experiments to indicate that change in friction does not coincide exactly with changes in mechanism state. [Rabinowicz 1951] found that the break-away transition from static to kinetic friction is not instantaneous. He defined the two temporal phenomena involved in stick-slip: rising static friction and frictional lag.

Based on these analysis and experimental results, we consider the one-dimensional model shown in Figure G.2. Velocity, $\dot{X}_d$, represents the relative velocity between the workpiece and the floor, K the stiffness of the robot and the workpiece, and b the damping of the robot. A typical force profile is shown in Figure G.3. This was obtained by sliding a flexible workpiece along a flat surface at a constant speed without vibration. The typical profile of a stick-slip force is shown in the interval from A to C in the figure. During the stick interval, A-B, the force rises at a rate proportional to velocity, $k\ \dot{X}_d$, and reaches the static friction at point B. Slipping occurs at interval B-C following the stick region. The exact motion is governed by the mass-spring dynamics as well as friction properties. As the speed increases, the magnitude of the maximum static friction force decreases. This stick-slip condition becomes significantly noticeable when there is a larger contact force or a higher coefficient of friction between the two contact surfaces. The ideal "smooth" contact is observed when the stick frequency approaches infinity and the amplitude approaches the nominal force. The sticking takes place while the horizontal force is less than the stiction, and slipping occurs when the internal stress force finally exceeds the stiction.

2.2 Assembly Using a Vibration Worktable

Our main goal is to develop an effective method to prevent sticking and jamming and allowing for smooth assembly operations. The technique we use is to generate dither: the one often used in parts feeders and servo controls. Instead of shaking the robot, we shake the worktable that holds a workpiece. We have found that robot actuators are not appropriate for generating dither due to limited durability and power. In contrast, worktables have less constraints and allow us to generate various dithering motions required for assembly tasks.

Figure G.4 shows the schematic design of the worktable considered in this paper. The system consists of an elastically supported platform, three independent solenoids that produce vibrating forces on the platform, and a robot manipulator equipped with a multi-axis force sensor. Each solenoid can generate various patterns of vibration with different frequency, amplitude, and phase. By changing combinations of frequencies and amplitudes of the three solenoids, we can create an arbitrary vibratory motion within a plane. The question is how to find an optimal combination and the optimal vibration modes of these parameters so that the sticking and jamming problems may be alleviated most effectively. The tuning of the three-axis vibrator comprises of many design parameters and depends upon many factors. Depending on the shape and size of the workpieces as well as their material and surface finish, optimal conditions of the vibrator will be different. Optimal parameters will also be different depending on the trajectory and compliance of the robot as well as the misalignment between the workpiece held by the robot and the one fixed to the worktable. These are all relevant factors and conditions, many of which are often unknown or uncertain. It is difficult to obtain a useful analytic model that predicts dynamic behavior of the workpieces and provides optimal conditions for the vibrator. In this

paper, we will develop an alternative approach to the optimal tuning; an experimental approach based on the Taguchi Method combined with a recursive optimization technique. First, we take data by having the robot perform a given task under various vibrator conditions. Task performance is evaluated using a performance index. Optimal ranges of parameters are then determined based on the performance index and the data acquired. Within the obtained optimal ranges, experiments are repeated to find better conditions in narrower parameter ranges. This cycle is repeated until the performance index reaches a satisfactory level. To make this operation effective, we need to reduce the number of experiments to be conducted and minimize human intervention in the optimization and data acquisition. We employ the Taguchi Method and develop an automated tuning system.

Chapter 3

Optimal Tuning using Taguchi Method

3.1 Traditional Learning Methods

The traditional learning methods require intensive human intervention in the preliminary planning that will enable the controller to "learn" or "acquire" the necessary human knowledge. Two of the most widely used learning algorithms are neural-network and fuzzy logic.

The neural-network functions in a way similar to how human neurons function. The multi-layer neural-network with backpropagation is an excellent method for learning and predicting a nonlinear function as long as a sufficient number of data points are collected from the system and the number of hidden layers and nodes of the network is above the minimum required for interpolating the system correctly. Up to now, there is still not a single rule or a guideline we can use to correctly pin down a minimum yet sufficient neural-network structure for each given system. Usually, some prior knowledge of the system is required simply to guess the behavior of the system. The network with its too simple structure can not converge and may stay at a local minimum. On the other hand, the network with a more complicated structure can be trained to follow the system smoothly. However, it undermines the noise effect when it is used to predict the outputs and requires a great deal of computation power and time.

The fuzzy logic method is based on the human linguistic rules or guidelines which form membership functions. Depending on the inputs of the system, particular rules

or guidelines are combined to give a single resultant output. It is this fuzziness output which gives merit to this method. Unlike binary logic, fuzzy logic also provides intermediate values between the two extreme values. However, performance of the method depends largely on the number of the linguistic rules and the shape of the membership functions. In order to define these correctly, the user must have an in-depth understanding of the system, usually up to the level of an expert, and needs to go through a time-consuming trial-and-error process to fine-tune the fuzzy controller.

The two methods mentioned above are both non-model-based methods which meet the general requirements described in Section 2.2. Both methods require an expert's knowledge in order to sufficiently transfer human skills to the controller. However, not all human "wisdom" is correct as some information may be missing. Therefore, much time is spent working with system identification and parameter estimation, in order to identify the factors that really affect the system or just to get some insights of the system before we can design the learning algorithm.

System identification deals with the problem of building mathematical models of dynamical systems based on the system data observed. The identification of models from the data involves decision making on the part of the person in search of models, as well as fairly demanding computations to furnish bases for these decisions. A user typically goes through several iterations in the process of arriving at a final model, revising earlier decisions at each step.

With a rigorous system identification method and after endless trial-and-error, the parameters involved in the system can be identified. However, the convergence still depends on the consistence of the data signals, and the original parameter structure. The user has to design both the actual planning and the trial-and-error processes. If every thing goes smoothly, the mathematical model will behave like the real system. However, the set of parameters obtained are considered to be the optimal solution only

to the particular output cost function used. It is not guaranteed that this solution is optimal for a different cost function.

The fine-tuning process of the controller as mentioned earlier requires extensive human intervention. Each data set collected from the system is incidental and subject to the noises that will arise from the system itself and the environment. After fine-tuning the controller to follow a certain data set, we will, most likely, have to redo the fine-tuning when another set of data is considered. Therefore, we may conclude that the controller is not flexible enough to gain on the overall picture. Besides the extensive fine-tuning processes, the preliminary planning of the project also requires human intervention. One practical way of using such a learning method is to combine it with an adaptive controller with a prior model built from the system identification method, as done in work by [Asada and Liu 1991]. However, the adaptive control is a model-based control, thus requiring us to provide an adequate model of the system. Extensive prior knowledge of the system is necessary for preliminary planning of the system.

The traditional intelligent learning methods require human expertise in designing the controller. This involves the design of learning strategies, applying them to experimental data to reduce the system and environment noises, and a final fine-tuning procedure to adjust the intelligent learning controller. At present, we still refer to systems with intelligent learning controllers as automated systems. However, if we consider the overall process as starting with the preliminary planning to the end when the output is obtained, human intervention plays a very important role in closing the control loop and supervising the controller action. In order to have a true automation process, we need to search for a new method to eliminate human involvement within the control loop. The Taguchi method, first developed by Dr. Genichi Tagauchi in the 1950s and 1960s, can provide the missing link between the human and the ma-

chine controller, thus eliminating the need for human involvement. Our next section will give a brief overview of the Taguchi Method.

3.2 Overview of the Taguchi Method

In Appendix C, we summarize the basic techniques of Taguchi Method, or Robust Design. Here, we will give a brief overview of the Taguchi method and its strengths in designing experiments. We see the Taguchi Method being applied to the product and process design in the industrial field. The attempt here is to apply this special discrete optimization method for the first time to the field of manufacturing control.

The key idea the Taguchi method, or Robust Design is to improve the performance of a system, or the quality of a product, by minimizing the effect of the causes of variation without eliminating the causes. This is achieved by optimizing the product and process designs to make the performance minimally sensitive to the various causes of variation [Phadke, 1989]. The Taguchi Method draws on many ideas from statistical experimental design to plan experiments for obtaining dependable information about the variables. Two major tools used in Robust Design are signal-to-noise ratio, which measures quality, and orthogonal arrays, which are used to study many design parameters simultaneously.

With the use of the orthogonal arrays, we can implement a minimum number of experiments in our design. Each different level of the control parameter appears an identical number of times during the entire experiment set when we use orthogonal arrays, thus enabling us to analyze the data with ease. Unlike the system identification process, there is no longer any human involvement in the experiment design. The preliminary planning process requires knowing only the number of control parameters and noise factors. The noise effects can be taken care of with another noise orthogonal array. Depending on the time and cost of the experiments, we can either have a

full-blown noise orthogonal array together with a regular control parameter array, which is usually used in simulated experiments; a single combined noise factor or no noise array, which is usually used for design process experiments; or a simplied noise orthogonal array at actual field noise level, which is used for the process experiments. In this way, the Taguchi Method has automated the preliminary planning process with the use of the orthogonal array. Thus the number of the experiments is guaranteed to be at a minimum and are robust enough to combat the effects of the noise.

With the use of the signal-to-noise ratio and analyses of mean and variance to the desired output, we can easily find the new optimal output setting in conjunction with the use of orthogonal arrays. Because each level of the control parameter appears the same number of times during the entire experiment, these analyses can easily find how each level of the control parameter affects the overall system. Based on the information from the current data set, the analyses give the optimal settings of control parameters for the next iteration. The analyses also indicate if any interactions between the control factors exist. Another advantage of the analyses is that the methods also indicate how strongly each factor affects the overall system. Thus, the analyses can instruct us as to which control parameters are unimportant enough to be eliminated and treated simply as system noise. The system now requires even fewer experiments because the size of the orthogonal array is reduced.

These analyses automatically spell out the desired output and give the direction to the next iteration while the modeled output given by the system identification method has to be interpreted by the user to see if it behaves like the true system output, and requires the search for a new setting, through guesswork and trial-and-error. Like the system identification method, fuzzy logic also requires human ability to analyze and find the new setting. The Taguchi Method, however, guarantees stability and convergence while the neural-network guarantees neither! The most remarkable

aspect of the Taguchi Method is that it takes the trouble and confusion out of the search for the new setting based on the massive system output.

The use of the orthogonal array lets us automate the experimental process through preliminary planning while the analyses offer the optimal control setting. Thus, with the use of the Taguchi Method, we have successfully taken the human factor out of the overall control loop. Because the Taguchi Method is a very systematic method, we can easily implement this method as shown in Figure G.10. In Section 3.3, we will apply this method to our optimal fine-tuning of the multi-axis vibrator.

3.3 Self-Tuning Procedure

We need to address the following questions found from our optimization method:

- How should we define the performance index that best quantifies the friction and the stick-slip condition?
- How can we apply this method most effectively to minimize our performance index?
- How should we generalize this procedure to make it autonomous and applicable to other assembly jobs?

We will address each of the questions in this section.

Assembly is the process of mating two workpieces together with geometric constrains. We define the ideal assembly process as a process when the workpiece is successfully inserted with a minimal number of intermediate steps and a minimal amount of time. Misalignment of the robot or workpiece, variations in parts, and jamming or wedging of the workpiece are some important reasons that increase the

number of intermediate steps and the amount of time required in the assembly process. Sometimes, if the misalignment is too great or the jamming or wedging is too severe, the assembly process will fail completely. The simplest and most cost-effective way of evaluating the assembly process is to keep track of the force information along the assembly process. For a given robot trajectory of an ideal assembly process, we define the ideal force trajectory as the summation of the static forces acting on the workpiece detected by the force sensor at each instantaneous time. As we deviate from the ideal case by adding friction, misalignment, variations in parts, wedging, or jamming to the assembly process, we start to observe variations in the force trajectory. As we improve the assembly process, we are in a sense, minimizing these variations. Thus we define our performance index as the summation of the root mean square force along the force trajectory. Eq. 3.1–Eq. 3.3 describe how we define them mathematically.

$$R(t) = (f(t) - m(t))^2 \tag{3.1}$$

$$T_r = \sum_{t=0}^{t=t_f} R(t) \tag{3.2}$$

$$m(t) = \frac{1}{n} \sum_{t=1}^{t=n} f(t) \tag{3.3}$$

where *R(t)* is the root mean square force at an instant time, *f(t)* is the force sensed at the force sensor, *m(t)* is the average dynamic force at an instant time, n is the size of the moving monitor window for evaluating Eq. 3.3, and the T_r is the summation of the root mean square force for the complete insertion process. We minimize this performance index in order to improve the assembly process.

In D. E. Whitney's paper, [Whitney, 1982], he uses the peak force value in the direction of insertion as his performance index. His main task is to perform one dimensional insertion of a cylindrical rod. The ideal force trajectory is a constant line along the direction of insertion. Thus we can treat the peak force at each instant time as a special case of the root-mean-square force. As described in [McCarragher and Asada, 1991], the assembly process is a discrete and dynamic process. Both the magnitude and the direction of the force vector vary quite significantly during the entire assembly process. The force trajectory does not stay constant as the complexity of the assembly process increases, but varies along the trajectory. Thus, looking only at the peak force value is not enough to describe a complicated assembly process. It is the variance from the dynamic mean of the force vector that best quantifies the friction and the stick-slip condition. Thus we define our performance index as the summation of the root-mean-square (RMS) force relative to its dynamic mean force, which is also known as the force trajectory. Our optimal solution, or the "smooth trajectory", should minimize this force variation.

Our main objective besides minimizing the friction and the stick-slip condition is to minimize the time and work necessary for the assembly system to arrive at an optimal value. In order to achieve these objectives, we used the experiment-based approach, Taguchi Method, as described earlier in Section 2.2 to obtain this optimal value. The Taguchi Method as based on [Phadke 1989] is described in detail in Appendix C.

(1) Minimizing Time and Work Required

Due to the use of orthogonal array in the Taguchi Method, the minimum number of the experiments we need to perform is $(m - 1) \times N$ where N is the number of control factors and m is the number of levels we wish to vary for each control factor.

However, if we use the conventional method, the minimum number of experiments we need to perform is m^N in order to have every single combinations possible. For example, if we have three levels for each of the six control factors, we need to run only 12 experiments if we use the Taguchi method instead of the 729 experiments required by conventional methods. Thus, the Taguchi Method saves both time and work in obtaining the optimal values, thus opening up the possibility of running these tests in real time.

(2) Minimizing the Cost Function, *S/N Ratio*

The Taguchi Method uses the Signal to Noise ratio (*S/N ratio*) as the main performance index to arrive at its optimal value. The S/N ratio is the ratio of the mean to the variance in decibel scale, which matches our definition of the performance index. Thus, by using the Taguchi method, we can minimize the friction and the stick-slip condition for assembly with a minimal number of tests.

From Appendix C, we see that the Taguchi Method is a very systematic and sequential method. In order to perform each iteration of the Taguchi Method, we need only to supply the following information:

1. Number of control factors (N)
2. Number of variant levels for each control factor (m)
3. Method selected to optimize the performance index:
   - **SIB** Small value is the best
   - **LIB** Large value is the best
   - **NIB** Nominal value is the best
4. The tolerance of the performance index

The method performs the analyses of the variance, mean, and interaction. The method determines the optimal settings based on the current experimental results. From ANORM, the method determines the relative setting of each factor by choosing the highest S/N point for each factor. By using the proportionality of each factor to the overall system in ANOVA, the method can reduce the number of the control factors, thus further reducing the number of the tests that need to be run for the next iteration and simplifying the control algorithm. The system runs a confirmation test based on the optimal setting to confirm the results.

(3) Automating the Taguchi Method

After completing the confirmation test, the method can be repeated for the whole process with a tighter bound around its newly arrived optimal settings than the previous iteration. However, only the ANOVA and ANORM tests need to be repeated since the interaction relationships remain unchanged. This iteration process is repeated until a satisfactory result within the specified tolerance is obtained.

This calibration procedure for the tuning of the multi-axis vibrator is autonomous throughout the entire process. The final optimal settings may be case sensitive for different kinds of assembly jobs. However, the calibration procedure is certainly universal for all assembly jobs. This self-calibration process can be "taught" to fine-tune the settings and adapt to a new assembly job by repeating this method.

Chapter 4

Implementation and Experiments

The experimental setup is described in Section 2.2. The vibrations are provided through three function generators to provide a precise vibration amplitude and frequency. Our first step is to demonstrate that vibration in general can reduce the possibility of stick-slip occurrence. The results show that we can effectively reduce RMS_{Mz} from 50 lb-in (0.576 Nm) for no vibration to 25 lb-in (0.288 Nm). Our next step is to fine tune the vibration system using the Taguchi Method to find the optimal setting for minimizing RMS_{Mz}.

4.1 Data Acquisition

The main purpose of this part is to detect the various slippage occurrences during the sliding motion. The construction of the pattern recognition is based on the flowchart shown in Figure G.6. The data is first acquired through actual experimental data. The pattern recognition is then done off-line. The pattern recognition program (PRP) will calculate the RMS F_x, F_y, and M_θ, and results are then fed into ANORM and ANOVA.

4.2 Orthogonal Array

The size of the orthogonal array is determined by the number of the control factors. In our case, we have a total of six control parameters: one input vibrating amplitude and frequency from each vibrator.

As described earlier, we performed an interaction test to check the correlation between the six factors. In order to study all six interactions, we chose a L_{32} 2-level orthogonal array for the interaction test presented in Figure G.7. Appendix A shows the results of our experiments. Appendix B shows the interaction plots for RMS_{M_z} for all six control factors. From the data, we see a strong correlation between F_{y1} and F_{y2} in the Y direction. This is in fact predictable since they both apply forces in the y-direction. The only difference between the two is in the direction of the applied moment.

Next, we assigned three levels to each control factor, one on the low, one in the middle and the last one on the high side from the norm. Based on the information given, we will choose L_{27} with 7 columns set as dummy columns since L_{27} was originally designed to accommodate 13 three-level control factors. The orthogonal array is shown in Figure G.9.

The output of the experiment is obtained from the previous pattern recognition program. Once we have all the information, we can start analyzing the data using *analysis of variance* (ANOVA) and *analysis of means* (ANOM).

4.3 Analysis of the Mean and Variance

The main purpose of this analysis is to estimate the effects that each factor has on the final results. First we must calculate the S/N ratio, η. Because the main purpose is to minimize the mean and the variance of the rms force and moments, we elect to compute the η based on the following equation which in turn is based on **SIB**, small is the best, principle.

$$\eta_i = -10log_{10}\left[\frac{1}{N}(\sum_{i=1}^{N}(y_i)^2)\right] \tag{4.1}$$

where **N** is the total number of experiments done for the particle set-up.

After we have computed the S/N value, we need to find the contribution of each level of a particular factor to the overall system. This is easily done by using the orthogonality of the orthogonal array and averaging the S/N values for the set-up for the same level of a particular control factor. Since we have 9 experiments per factor level, the S/N mean for a level A_1 is calculated as follows:

$$m_{A_1} = \frac{1}{9}\left(\sum_{i=1}^{n} m_i\right) \tag{4.2}$$

Results of the factor level contribution are given in Appendix C. The one with the highest S/N value of each factor is the one that is least sensitive to noise. The combination of $Xamp_1 - Xfre_2 - Y1amp_1 - Y1fre_3 - Y2amp_2 - Y2fre_2$ gives the highest S/N value.

The next step is to find out how each factor affects the overall system. To do so, we simply sum the variance of factor level mean to the overall mean for each factor. For example, the contribution of Xamp is

$$Var_{Xamp} = 9*(Xamp_1 - mean)^2 + 9*(Xamp_2 - mean)^2 + 9*(Xamp_3 - mean)^2 \tag{4.3}$$

9 represents the nine experiments done for each factor level. The ratio of each factor variance to the total variance is the contribution or effect of a particular control factor on the total system. In our case, *Y1 amp* can take on the highest variation with 81% followed by Xamp with 8.54%. We can then estimate the optimal S/N value, η_{opt}. η_{opt} is calculated based on the total mean and the difference in contributions from the upper half of the control factors to the mean. This value of η_{opt} is then used to do linear interpolation to find the optimal setting for each of the control factors. The η_{opt} value in our case can be calculated by the following equation:

$$\eta_{opt} = \eta_{mean} + (\eta_{Xamp} - \eta_{mean}) + (\eta_{Y1amp} - \eta_{mean}) + (\eta_{Y2fre} - \eta_{mean}) \quad (4.4)$$

We can then convert this η_{opt} back to the estimated RMS_{Mz} value as follows

$$RMS_{Mz} = \sqrt{10^{-\frac{\eta_{opt}}{10}}} \quad (4.5)$$

Our η_{opt} value is -21.05 dB, which gives the RMS_{Mz} value of 0.0886 lb-in (0.00102 Nm). Our next step is to run a confirmation test to confirm the test results. Our confirmation test shows a final RMS_{Mz} value of 1.5 lb-in (0.0173 Nm). If we want to further reduce this value, we can repeat the overall process with a band around the optimal setting that is tighter than what we selected from our previous test results.

4.4 Interpretation of the test results

The test results show a 50% reduction in RMS_{Mz} from 50 lb-in (0.576 Nm) where no vibration is applied, to an average of 25 lb-in (0.2880 Nm). After the first iteration by the Taguchi Method, the value was further reduced to 10 lb-in (0.115 Nm). The confirmation test based on the optimal setting from the first iteration has reduced the RMS_{Mz} value to 1.5 lb-in (0.0173 Nm). The RMS_{Mz} value is the criteria we use to evaluate stick-slip, and therefore, by lowering RMS_{Mz}, we can have a much smoother assembling process which means a lesser chance of stick-slip.

In order to smooth out the motion in the **Y** direction, we need vibration forces in the **X** and **Y** directions together with a moment in the **Z** direction. The applied moment in each instance opens the gap between the two contacting surfaces thus allowing less chance for the workpiece to stick. An interesting fact is that we need the moment and its frequency but not its magnitude to reduce the sticking or to keep it from occurring altogether.

4.5 Automation of the Taguchi Method

The Taguchi Method is a very systematic sequential method. It can be modified quickly into a learning scheme by using the flowchart shown in Figure G.10. In fact, this is how we obtained our optimal input settings except we have human intervention instead of total automation. By having the user enter the number of control variables and guess the initial optimal settings, the computer then searches for the right orthogonal array to use. The range of the initial settings is based on the initial intuition of the user. Then the computer performs the experiments. The force data are obtained directly through the robot force sensor. The two analyses are performed. After each iteration, the computer runs a verification test to validate the newly arrived optimal settings. Before the optimal settings are set to start another iteration, the computer checks the relative contributions from each factor to see if reduction on the number of the control factors is possible. The process is repeated until the final optimal result falls within the tolerance.

Chapter 5

2-D Cable Connector Insertion

After seeing how the Taguchi Method has successfully reduced the stick-and-slip condition in one-dimensional sliding, we apply a completely automated method to do a more realistic and complicated 2-D insertion of a cable male connector to its female counterpart as shown in Figure G.13. The hardware and software issues will be introduced later in this chapter. The experimental results will be presented as well.

5.1 Hardware Setup

The robot used in the experiment is the *PanaRobo A3* manufactured by *Panasonic Inc.* as shown in Figure G.12. It has four degrees of freedom: X, Y, Z, and θ. In this implementation, experiment, we deal only with planar insertion. The robot moves in the X, Y, and θ directions to complete the insertion.

The complete experimental setup is shown in Figure G.11. The workpiece used in these experiments is a 25-pin male cable connector, the RS232 Mini-Tester. Our goal is to insert this 25-pin male cable connector into its female counterpart, both of which are shown in Figure G.13. The multi-axis vibration table shown in the previous chapter is also used for this experiment.

The J_3 force sensor is mounted on the wrist of the robot. This sensor can measure forces and moments in all directions. In this case, we shall use only the F_x, F_y and M_y variables so as to adapt to the setup. The control console is controlled by an IBM-

compatible Dell computer which runs at 25 Mhz. The control commands are sent directly through the control board of the robot which has its own built-in position control algorithm. This may create a jiggling motion in the robot and has a dominant effect on the force sensing data and the smoothness of the robot motion.

5.2 Software Setup

The source code of this software program is written in *Microsoft C* and is based on the flowchart shown in Figure G.10. The main program must perform the following tasks:

- Design an appropriate orthogonal array for the experiments
- Run the experiments according to the assigned orthogonal array
- Calculate the root mean square force values with respect to the dynamic mean
- Perform ANOVA and ANORM analyses to find the new optimal values and settings
- Repeat the process using newly assigned settings until performance is at an acceptable level.

More detailed descriptions and the issues involved are presented below.

(1) Preliminary Planning

The preliminary planning segment of the program asks the user for the number of the inputs and the control parameters. Then it assigns an appropriate orthogonal array based on the number of input control parameters. The main purpose of this segment of the program is to design and plan a strategy for the experimental set-up so that the

controller can understand the system after running a minimum number of experiment sets. The sets of orthogonal arrays used here are all standard ones. Appendix E shows two of the orthogonal arrays used for the experiments. This program has been written to accept three to six three-level control parameters. The program assigns a L_9 orthogonal array to a system with three or four control parameters and a L_18 orthogonal array to a system with five or six control parameters. The user also enters a maximum allowable performance index tolerance so that the program will terminate after it arrives within the specified window. The user is also required to enter the maximum number of iterations just in case the program does not reach the specified tolerance within a reasonable time interval.

(2) Data Acquisition

The main tasks of the data acquisition segment of the program are to send amplitude and frequency values to the vibrators and to move and control the robot while it takes force and position data. These tasks can be found in Figure G.14. Due to the present limitations of hardware in the computer architecture, the vibration commands can not be sent directly to the vibrators; instead, they are presented on the screen and require human aid to set them up. Even though the controller requires human intervention, it does not require a decision on the part of the human. The robot motion is predetermined and the controller performs a very simple trajectory control in conjunction with the logical branching [Li, 1991]. The robot motion follows a trajectory as shown in Figure G.15. A simple logical branching algorithm is added to the control loop monitoring robot motion. The purpose of the logical branching algorithm is to ensure that the robot reaches a specified contact state or remains at that state, but does not arrive at a danger contact state. Our main purpose is to use the robot to acquire data. Therefore, the robot trajectory control algorithm is kept

at minimal complexity. All the force and position data of each experiment are stored in different files. Approximately 600 to 700 sets of data are collected during each trial and the sampling time is approximately 2ms.

(3) Evaluating the Performance Index

The performance index as defined earlier is the minimum root mean square forces. Our first step is to define how we actually obtain the values of the root mean square force in this case. In order to ensure that the root mean square values we obtain are valid, we must look into the force trajectory. A simplified definition of the force trajectory is found by taking the instantaneous values of the dynamic mean or average force value within a moving monitor window. The square variation from the mean is our definition of the root mean square. An important issue here is how to determine the size of the dynamic monitor window. An appropriate window size captures the true force variation without concerns about whether it is too sensitive or too static to the changes in force data. A typical force data plot and its force trajectory is plotted in Figure G.16. We find that the ideal size of a dynamic monitor window that will give the most accurate values of the root mean square is 100. After the robot switches contact states, the dynamic mean values are recalculated based only on the force data obtained at the new contact states to ensure their validity.

(4) Minimizing the Performance Index

The analyses of the mean and variance segment of the program are exactly the same as those presented in Section 4.3. The final optimization segment of the program is also similar to the material presented in Section 4.3. The program assigns different new settings for each level. This is done to ensure that the final optimal value is an absolute and not a local minimum. If the signal-to-noise ratio is highest for either

the lowest or highest level of a particular control parameter, the three new settings are shifted by a distance from that level to the original mean, with no change in the variance. On the other hand, if the central setting gives the highest signal-to-noise ratio, it remains at its previous position and the variance is cut down to half of its original magnitude. This whole process is repeated until the root mean square forces reach an acceptable level.

5.3 Experimental Results

Before we run the entire program, we first obtain two data sets. The first data set is found by running the robot through the trajectory without making any contact as shown in Figure G.17. The second data set is obtained by running the robot through the trajectory without vibration as shown in Figure G.18. Figure G.19 shows the force and position plot obtained by using the optimal settings obtained after the first iteration of the Taguchi experiment set. The first complete experimental analysis is presented in Appendix F. After completing the first iteration, we have effectively reduced the magnitude of the peak force by half by switching from random vibration to tuned vibration. We have also reduced the peak root mean square force and moment from 10.545 lb for no vibration to 2.5 lb for untuned vibration, and 1.5 lb for tuned vibration after the first iteration.

We have shown here that the Taguchi Method works for two dimensional cable insertion. However, instead of a single force performance index as for the case of one dimensional insertion, we now have three performance indices (root mean square force in the X and Y directions and Moment in the Y direction). At present, we treat them as three separate performance indices in our analyses. Fortunately, they predict the same settings for all output parameters except one in spite of different output signal-to-noise ratios. We need to direct our work toward background research and

finding a Taguchi optimization for multiple performance indices.

In the previous chapter, we describe the basic methodology and how it can be applied through a very simple and primary case study of 1-D sliding. In order to apply the same Taguchi Method to the 2-D cable connector assembly process, we must clarify the definitions and assumptions used.

The experiments are run under several assumptions, which are fixed robot trajectory, fixed contact states, and no variations in parts. However, small variations in trajectory are unavoidable when the experiments actually take place. At present, we treat any unavoidable or uncontrollable variations as built-in noises. If time is allowed, a more robust orthogonal array should be implemented. Besides using an orthogonal array for the control parameters, we should also incorporate a noise orthogonal array to account for any "noise" we encounter in case of misalignment, variation in workpieces, and so on. However, we may sacrifice efficiency by requiring more experiments. The optimalization we arrived at is then optimized globally. At present, the optimization is obtained off-line and can not respond to any spontaneous change or variation. In order to obtain a more robust algorithm, we will implement a hybrid controller which will use the Taguchi Method to obtain off-line optimized settings and the learning algorithm to optimize on-line variations. The Taguchi Method can provide a excellent starting point for on-line learning and training, thus eliminating the need for blind guesses.

Chapter 6

Conclusion and Future Work

In the manufacturing process utilizing robotic precision assembly today, stick-slip condition and jamming have severely limited the rate of robot assembly. Due to the complexity of the assembly task, force control itself is not totally effective in a complex assembling process. The visual systems help but have proven to be too slow and expensive. In order to reduce the chance of jamming and sticking, we tried to use a multi-axis vibrator together with passive compliance built into the worktable. The primary reason for adding both the compliance and vibration to the worktable is so that we will not complicate the original system while effectively reducing both detrimental effects.

The new contribution that we make here is to bringing the true meaning of automation to reality, unlike the past, when the automated system was defined as a system that could perform its duty without human supervision. The advance in artificial intelligence (AI) is what makes this possible. The most frequently used AI techniques are neural-network, fuzzy logic, and the expert system. In order to apply these intelligent control algorithms to the design of a control system, a great amount of man-power is spent to understand the system, to acquire knowledge from experts, to analyze data, and most importantly, to go through an almost endless trial-and-error process once the controller is built. Sometimes, a hybrid controller is constructed by combining the intelligent controller together with an adaptive controller that uses a system identification technique. If we step up one layer and look at an overall picture of the automation system by considering all the processes that require human inter-

vention as part of the so-called automation process, we soon realize that the human factor acts either as a black box to close the old definition of an automated controller, or acts as God to supervise or oversee the overall control system. Therefore, the automation process defined earlier can only be considered as a semi-automated process. This new process, the Taguchi Method, replaces the human role in the overall control picture and brings true meaning to the automation process. The use of the orthogonal array in planning the strategy for understanding the system keeps the amount of time and the number of experiments required at a minimum. With the analyses of the mean and variance, the system obtains settings that give better performance. By repeating this process, the system can obtain optimal settings for its control parameters. Therefore, there is no human involvement in the decision making process. We now have a true automation process with machine intelligence obtained by the machine itself not by a human.

Instead of using a model-based approach to control the multi-axis vibrator, we use an experimental approach based on the Taguchi Method. The problem with a model-based design is the complexity of equations where many assumptions have to be taken in order for the model to behave like a real system. However, many of the disturbances or non-modeled factors may still destroy the reliability of the model when the model meets the challenge of the real system. With the help of the Taguchi Method, we can find an optimal solution with a very limited number of experiments to reduce stick-slip condition with a strong ability to reject outside noises. In comparison with other experimental approaches the Taguchi Method guarantees convergence as compared to the neural-network method, involves less guesswork than fuzzy logic, and does not require as many experiments as Monte-Carlo's method.

The use of vibration has effectively reduced 50% of the RMS_{M_z} value from 50 lb-in (0.576 Nm) to an average of 25 lb-in (0.288 Nm). After the first iteration by the

Taguchi method, it was further reduced to 10 lb-in (0.115 Nm). The confirmation test based on the optimal setting from the first iteration has reduced the RMS_{Mz} to 1.5 lb-in (0.0173 Nm). The RMS_{Mz} value is the criteria we used to evaluate stick-slip and by lowering RMS_{Mz}, we can have a much smoother assembly process which means a lesser chance of stick-slip and jamming.

We also demonstrated automated methodology in the use of a more complicated system—two dimensional cable connector insertion. The repeatability and reliability of the insertion process have been greatly improved, and our next step is to generalize the methodology to perform optimization of a system with multiple performance indices. In order to build a more robust controller, we need to implement a hybrid controller. However, more research work need to be undertaken in future studies combining the off-line tuning using the Taguchi Method and on-line tuning using learning methods.

Appendix A

Experimental Results of L_{32}

Data	xrms	yrms	zrms	Data	xrms	yrms	zrms
Data1_1	0.631600	0.386220	33.449450	Data17_1	3.305852	0.253059	43.050006
Data1_2	0.745926	0.401373	42.437390	Data17_2	1.953383	0.335564	22.798210
Data1-3	0.533244	0.326157	30.354020	Data17-3	1.460050	0.387565	16.587378
Data1-4	0.469799	0.399991	24.883670	Data17-4	1.413327	0.303531	15.266325
Data3_1	0.669109	0.495550	33.416890	Data19_1	0.629917	0.539315	34.764690
Data3_2	0.639030	0.335623	35.942300	Data19_2	1.208122	0.962160	88.251120
Data3-3	0.487262	0.344898	30.105760	Data19-3	0.920129	0.574406	6.567560
Data3-4	0.546419	0.309265	20.017820	Data19-4	0.925985	0.431937	60.655120
Data5_1	0.800507	0.286761	40.603010	Data21_1	3.560699	0.602823	48.845657
Data5_2	3.318488	55.184784	40.584564	Data21_2	3.569572	0.618212	54.496500
Data5-3	0.570114	0.170395	29.120340	Data21-3	2.125860	0.317944	29.524176
Data5-4	0.496368	0.216509	25.162730	Data21-4	2.042527	0.379212	31.324150
Data7_1	2.729831	49.571873	43.813393	Data23_1	0.692088	0.378687	51.508930
Data7_2	0.764962	0.379940	51.117550	Data23_2	0.733450	0.386313	43.974640
Data7-3	0.538099	0.297763	24.446380	Data23-3	0.543610	0.259344	32.554280
Data7-4	0.628073	0.376220	37.941460	Data23-4	1.054100	0.298853	89.733850
Data9_1	1.806185	1.773521	87.385700	Data25_1	0.789585	0.356599	57.399760
Data9_2	0.593186	0.402782	27.428150	Data25_2	0.733450	0.386313	43.974640
Data9-3	0.564587	0.283399	32.497720	Data25-3	0.543610	0.259344	32.554280
Data9-4	0.561635	0.380465	31.147540	Data25-4	1.054100	0.298853	89.733850
Data11_1	0.633752	0.414638	26.366620	Data27_1	2.784378	0.565457	30.829151
Data11_2	0.724103	0.478380	24.197010	Data27_2	1.575221	3.331307	22.195351
Data11-3	0.515954	0.325968	27.456240	Data27-3	1.892658	0.533320	23.060593
Data11-4	0.593478	0.379757	31.187770	Data27-4	12.362161	66.581535	11.173395
Data13_1	0.794202	0.426320	35.498815	Data29_1	3.200601	0.498824	45.248123
Data13_2	1.578377	0.464028	17.048122	Data29_2	3.357237	0.472298	45.223053
Data13-3	42.593395	218.632629	37.064381	Data29-3	2.663130	0.305415	34.914165
Data13-4	0.698332	0.410019	72.590510	Data29-4	2.256656	0.268436	32.921432
Data15_1	1.116601	0.834322	103.751420	Data31_1	0.991634	0.286065	47.295630
Data15_2	1.187962	0.580639	101.417490	Data31_2	1.031742	0.206514	68.131520
Data15-3	0.962306	0.390042	78.180450	Data31-3	1.071779	0.694098	45.037860
Data15-4	1.099293	0.306379	62.938790	Data31-4	0.691289	0.311682	45.406360

Appendix B

Interaction Results for RMS_{Mz}

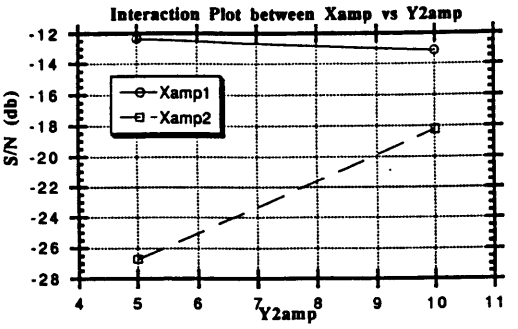

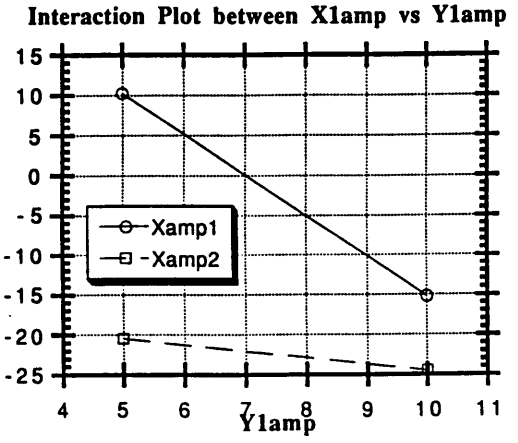

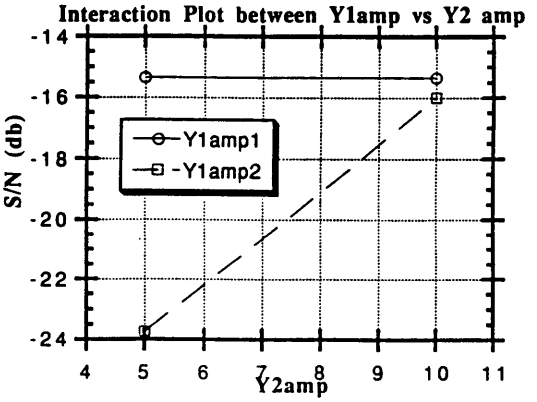

Appendix C

Experimental Result and Analysis of L_{27}

Exps	Rms Fx	Rms Fy	Rms Mz	S/N Fx SIB	S/N Fy SIB	S/N Mz SIB
1	1.966205	0.545727	11.891223	-5.872576	5.260491	-21.504530
2	2.267037	0.799998	13.149055	-7.109172	1.938222	-22.377891
3	2.168582	0.747055	14.207358	-6.723517	2.532948	-23.050266
4	2.292162	0.873456	12.783412	-7.204906	1.175179	-22.132936
5	1.861696	0.532458	13.010080	-5.398175	5.474293	-22.285599
6	2.178602	0.582816	14.499487	-6.763558	4.689371	-23.227053
7	2.176113	0.516702	11.248361	-6.753629	5.735197	-21.021785
8	2.214705	0.922260	14.059573	-6.906318	0.702933	-22.959443
9	2.058663	0.704398	15.753448	-6.271705	3.043638	-23.947512
10	2.181564	0.530046	11.724640	-6.775359	5.513729	-21.381990
11	3.051816	0.787758	15.262383	-9.691167	2.072144	-23.672447
12	2.422783	0.715203	14.849022	-7.686290	2.911413	-23.433957
13	1.890541	0.700058	10.860065	-5.531722	3.097320	-20.716648
14	2.210976	0.667659	14.916417	-6.891681	3.508906	-23.473290
15	3.594397	1.085750	15.424112	-11.112521	-0.714597	-23.764003
16	1.951965	0.443113	12.225275	-5.809441	7.069710	-21.745173
17	2.388404	1.198718	15.255977	-7.562156	-1.574341	-23.668801
18	2.139034	0.623594	13.937175	-6.604354	4.101961	-22.883495
19	2.129119	0.762147	13.407932	-6.563999	2.359225	-22.547236
20	2.793014	0.693648	15.597404	-8.921462	3.177217	-23.861046
21	2.523772	1.050106	15.644770	-8.041002	-0.424663	-23.887384
22	1.960492	0.629897	11.144692	-5.847301	4.014609	-20.941361
23	3.665038	0.824401	16.549311	-11.281570	1.677230	-24.375598
24	2.069174	0.688617	14.213817	-6.315940	3.240445	-23.054214
25	2.411952	0.498468	12.914556	-7.647373	6.047254	-22.221590
26	2.343889	0.898450	16.381378	-7.398741	0.930122	-24.287009
27	2.643202	0.797347	15.296910	-8.442607	1.967053	-23.692074
Mean	2.353885074	0.734068519	13.93362344	-7.301046	2.945445	-22.819049

Inv Fac	Fx	Fy	Mz
X amp 1	-5.859094566	3.056514912	-22.50077951
X amp 2	-8.215155014	3.225542577	-22.7488672
X amp 3	-7.828888424	2.554276948	-23.20750141
X fre 1	-7.487171646	2.815636326	-22.85741646
X fre 2	-7.371930473	2.906972859	-22.66341157
X fre 3	-7.044035885	3.113725252	-22.93632009
Y1 amp1	-6.445145119	4.474746089	-21.57924996
Y1 amp 2	-7.836203183	2.249714467	-23.54991043
Y1 amp 3	-7.551277198	2.371952234	-23.43777327
Y1 fre 1	-7.015692653	3.700189223	-22.75976977
Y1 fre 2	-8.111751616	1.853516873	-23.08418943
Y1 fre 3	-6.775693734	3.282628341	-22.61318892
Y2 amp1	-7.12244726	3.656280605	-22.89903628
Y2 amp2	-7.791584779	3.694995948	-22.77168911
Y2 amp3	-6.989105965	1.485057884	-22.78642273
Y2 fre 1	-7.001570128	2.930957496	-22.7268039
Y2 fre 2	-6.909421905	3.334161556	-22.60902866
Y2 fre 3	-8.192893844	2.093536104	-23.10435294
Factor Xamp	28.74093167	2.194232609	2.314046023
Factor Xfre	0.951494073	0.419837765	0.355028205
Factor Y1amp	9.734176626	28.36527163	22.08671749
Factor Y1fre	9.131986188	16.88074635	1.045726636
Factor Y2amp	4.618386859	14.66047201	0.097955052

Xamp %	45.97%	3.12%	8.54%
Xfre %	1.52%	0.60%	1.31%
Y1amp %	15.57%	40.28%	81.48%
Y1fre %	14.61%	23.97%	3.86%
Y2amp %	7.39%	20.82%	0.36%
Y2fre %	14.95%	11.21%	4.45%
Nopt	-5.895042	5.979042	-21.050959
RMS	0.507280	1.990454	0.088604

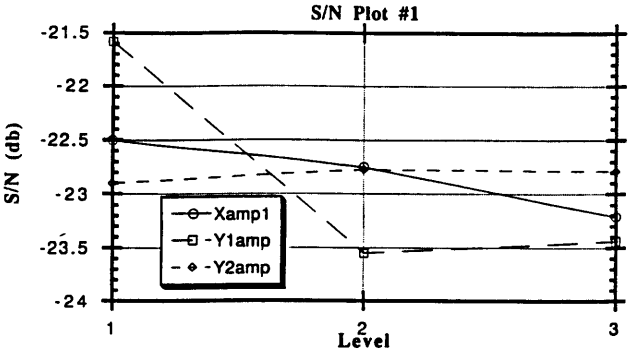

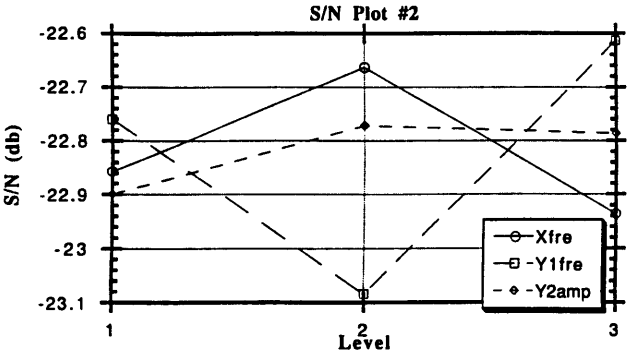

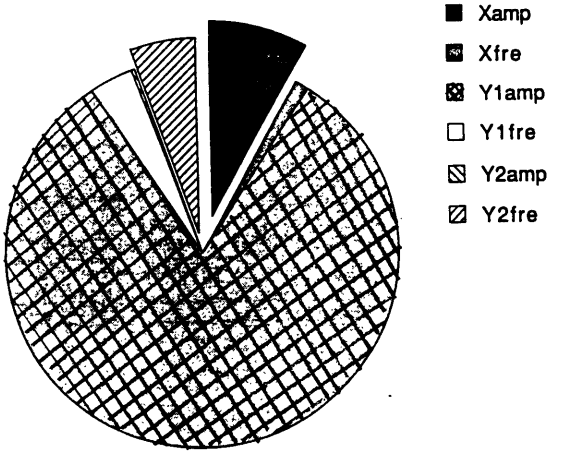

Effectiveness of each control factor has on the total system

Appendix D

Taguchi Method [Phadke, 1989]

Referring to [Phadke, 1989], we summarize the basic techniques of Taguchi Method, or the Robust Design, to be used for tuning the vibratory table. The key idea behind the Robust Design or the Taguchi Method is to improve performance of a system, or the quality of a product, by minimizing the effect of the causes of variation without eliminating the causes. This is achieved by optimizing the product and process designs to make the performance minimally sensitive to the various causes of variation [Phadke, 1989]. The Taguchi Method draws on many ideas from statistical experimental design to plan experiments for obtaining dependable information about the variables. Two major tools used in Robust Design are signal-to-noise ratio, which measures quality, and orthogonal arrays, which are used to study many design parameters simultaneously.

The technique referred to as Parameter Design helps to reduce the sensitivity of output to the noise factors of the system. A typical example of system signal input and output is shown in Figure G.5. The signal factors ($\mathbf{M}$) are the factors set by the user to express the intended value for the response of the product. The response factors ($\mathbf{y}$) are the output of the process which we want to improve. The control factors ($\mathbf{z}$) are factors that can be changed freely by the user. They are selected to minimize the sensitivity of the product's response to all noise factors. The noise factors are factors which can not be controlled by the users. These may either be the factors the user has no control over such as external disturbances or the factors the

user decides not to control due to the fact the influences of such factors are negligible.

In order to plan effectively for the parameter design we have to make use of orthogonal arrays. Once we determine the number of factors involved, the levels in which we want to vary a particular factor, the number of 2-factor interactions to be estimated, and the difficulties in running the experiments, we can then determine the size of the orthogonal array. As the name suggests, the columns of the array are mutually orthogonal. For any pair of columns, all combinations of factor levels occur and they occur an equal number of times. Based on the orthogonality, we can then easily find how each level of a particular factor affects the total system.

The main purpose of this analysis is to estimate the effects that each factor has on the final results. First we have to calculate the signal to noise (S/N) ratio, η. We then calculate the mean of η and the means of the results to find its effect on each factor level. The one with the highest mean for a given control factor is chosen due to the fact that it has the highest S/N ratio, or, in other words, is most robust. We then use the *analysis of variation* ANOVA to analyze the contribution of each factor.

Analysis of variance (ANOVA) is a mathematical technique which breaks the total variation down into accountable sources; the total variation is decomposed into its appropriate components. It is based on the least squares approach; the error variance is equal to the minimum value of the sums of squares about some reference divided by the degrees of freedom for error. A degree of freedom in a statistical sense is associated with each piece of information that is estimated from the data.

The basic property of ANOVA is that the total sum of square is equal to the sum of the sums of square due to the known components.

$$SS_T = SS_m + SS_e \tag{D.1}$$

where SS_T is the total sum of squares, SS_m is the sum of squares to the mean, SS_e is error sums of squares. Sums of squares can be written as

$$SS_T = \sum_{i=1}^{N} y_i^2 \tag{D.2}$$

which is the summation of the squares of each observation from i=1 to N, and

$$SS_m = \frac{T^2}{N} \tag{D.3}$$

where T is sum of all observations and N is the total number of observations.

Based on the above equations, we can find out the sum of squares for a particular factor in the system

$$SS_A = \sum_{i=1}^{N} n_{A_i} \left(\bar{A}_i - \bar{T}\right)^2 \tag{D.4}$$

where SS_A is the sum of squares due to Factor A, n_{A_i} is the total number of observations at each particular level for Factor A, $\bar{A}_i$ is the average value for Factor A at the ith level, and $\bar{T}$ is the average value for the overall system. By completing Eq. D.4 for all the factors, we can then determine the proportion of influence of this particular factor on the overall system.

We then used the sum of squares corresponding to the lower bottom portion of the factors and to about half of the degrees of freedom used to estimate the error mean square or error variance. By comparing this lower half to each of the control factors from the upper level we can decide which control factor has the greatest contribution. If this proportion is very large, we can reduce the total number of control factors and treat them as the noise of the experiments. The error variance ratio (σ_e^2) is calculated based on the ratio of the sum of squares due to error to the degrees of freedom for the error. η_{opt} is calculated based on the total mean and difference contributions from

the upper half of control factors to the mean. This value of η_{opt} is then used to do linear interpolation to find the optimal setting for each of the control factors.

Based on the orthogonal array, we should have independent control factors. The results of one factor should be independent of the others. However, due to the nature of the actual physical system, the control factors chosen may physically interact with one another. So, first we need to check if there exists any interaction between any two control factors.

Table 1 Interaction of Two Factors

	A_1	A_2
B_1	A_1 x B_1	A_2xB_1
B_2	A_1 x B_2	A_2 xB_2

where A_1xB_2 represents the iteration between A_1 and B_2. We can rewrite Eq. D.1 by adding the interaction term

$$SS_T = SS_A + SS_B + SS_{AxB} + SS_e \tag{D.5}$$

The sum of squares for Factor A or B can be calculated as follow:

$$SS_A = \frac{(A_1 - A_2)^2}{N} \tag{D.6}$$

The interaction can be calculated from Eq. D.1

$$SS_{AxB} = \left[\sum_{i=1}^{c}\left(\frac{(AxB)_i^2}{n_{AxB_i}}\right)\right] - \frac{T^2}{N} - SS_A - SS_B \tag{D.7}$$

After plotting out the interaction plot between the two factors, we can find that the slopes of the lines change from one level to another, thus proving that the two factors are correlated.

Appendix E

The Orthogonal Array Used

E.1 The Standard L_9 Orthogonal Array

This orthogonal array is used for any system with up to 4 control parameters. Each of them have 3 levels.

No.	val1	val2	val3	val4
1	1	1	1	1
2	1	2	2	2
3	1	3	3	3
4	2	1	2	3
5	2	2	3	1
6	2	3	1	2
7	3	1	3	2
8	3	2	1	3
9	3	3	2	1

E.2 The Standard L_{18} Orthogonal Array

This orthogonal array is used for any system with up to eight control parameters with seven three-levels and one two-level control parameters.

No.	val1	val2	val3	val4	val5	val6
1	1	1	1	1	1	1
2	1	2	2	2	2	2
3	1	3	3	3	3	3
4	2	1	1	2	2	3
5	2	2	2	3	3	1
6	2	3	3	1	1	2
7	3	1	2	1	3	2
8	3	2	3	2	1	3
9	3	3	1	3	2	1
10	1	1	3	3	2	1
11	1	2	1	1	3	2
12	1	3	2	2	1	3
13	2	1	2	3	1	2
14	2	2	3	1	2	3
15	2	3	1	2	3	1
16	3	1	3	2	3	2
17	3	2	1	3	1	3
18	3	3	2	1	2	1

Appendix F

Cable Insertion Experimental Data

The followings are the summary charts from the first iteration set of the cable insertion experiments.

This is the L18 orthogonal array

No.	val1	val2	val3	val4	val5	val6
1	1	1	1	1	1	1
2	1	2	2	2	2	2
3	1	3	3	3	3	3
4	2	1	1	2	2	3
5	2	2	2	3	3	1
6	2	3	3	1	1	2
7	3	1	2	1	3	2
8	3	2	3	2	1	3
9	3	3	1	3	2	1
10	1	1	3	3	2	1
11	1	2	1	1	3	2

12 ||	1	3	2	2	1	3
13 ||	2	1	2	3	1	2
14 ||	2	2	3	1	2	3
15 ||	2	3	1	2	3	1
16 ||	3	1	3	2	3	2
17 ||	3	2	1	3	1	3
18 ||	3	3	2	1	2	1

These are the values assigned to the L18 orthogonal array

No.	val1	val2	val3	val4	val5	val6
1 ||	6	8	6	8	6	8
2 ||	6	10	8	10	8	10
3 ||	6	12	10	12	10	12
4 ||	8	8	6	10	8	12
5 ||	8	10	8	12	10	8
6 ||	8	12	10	8	6	10
7 ||	10	8	8	8	10	10
8 ||	10	10	10	10	6	12
9 ||	10	12	6	12	8	8
10 ||	6	8	10	12	8	8
11 ||	6	10	6	8	10	10
12 ||	6	12	8	10	6	12

13	8	8	8	12	6	10
14	8	10	10	8	8	12
15	8	12	6	10	10	8
16	10	8	10	10	10	10
17	10	10	6	12	6	12
18	10	12	8	8	8	8

This is the original RMS output

No.	RMS Fx	RMS Fy	RMS Mz
1	1.451114	1.457039	1.934590
2	0.134439	0.136211	0.178621
3	1.060358	1.075793	1.087254
4	0.266329	0.288692	0.347124
5	0.291848	0.298687	0.495710
6	0.177884	0.177970	0.179568
7	0.380949	0.388595	0.381166
8	0.203055	0.206745	0.314876
9	0.535551	0.550968	0.565483
10	0.895775	0.909958	0.901830
11	1.463593	1.468011	1.678412
12	0.734646	0.734649	0.734830

13	1.321949	1.327084	1.322688
14	0.385387	0.386576	0.388823
15	2.235833	2.239535	2.245966
16	0.118833	0.119324	0.118876
17	2.258224	2.302106	2.389546
18	0.487156	0.494377	0.527920

Variables with S/N value

==========

S/N Fx

No.		val1	val2	val3
1	||	14.01246	36.05474	45.32693
2	||	33.67325	39.87240	21.84848
3	||	-3.69095	43.00981	56.07528
4	||	31.36619	56.95976	7.06818
5	||	18.78976	49.82983	26.77454
6	||	13.10069	53.57798	28.71546

S/N Fy

No.	val1	val2	val3
1	13.57515	35.07422	44.42060
2	32.55899	39.18094	21.33004
3	-4.88090	42.36075	55.59011
4	30.97325	55.93905	6.15767
5	18.39287	48.47824	26.19885
6	12.33897	53.19177	27.53923

S/N Mz

No.	val1	val2	val3
1	7.57875	28.94892	39.84698
2	28.80272	27.23469	20.33725
3	-10.68220	35.23026	51.82659
4	26.81699	48.33518	1.22249
5	11.90166	43.75437	20.71862
6	4.73336	49.82548	21.81581

New values based on Fx are following:

Var	LOW	MEDIUM	HIGH

1	8	10	12
2	9	10	11
3	8	10	12
4	9	10	11
5	7	8	9
6	9	10	11

New values based on Fy are following:

Var	LOW	MEDIUM	HIGH
1	8	10	12
2	9	10	11
3	8	10	12
4	9	10	11
5	7	8	9
6	9	10	11

New values based on Mz are following:

Var	LOW	MEDIUM	HIGH
1	8	10	12
2	6	8	10
3	8	10	12
4	9	10	11

```
     5       7       8       9
     6       9      10      11


Contribution from each factor

============================

    Var  S/N Fx        S/N Fy         S/N Mz

=========================================

     1 1007.320250   965.522835   743.895083
     2 890.729678    853.032515   577.784712
     3 1493.013355   1472.470024  1263.234175
     4 1249.782722   1211.776506  935.120217
     5 1008.026630   961.237017   744.593844
     6 1112.647527   1082.972189  909.779634


Contribution from each factor expressed in percentages

=====================================================

     Var   Fx per        Fy per       Mz per

=============================================

     1   14.8978370   14.7475363   14.3764297
     2   13.1735121   13.0293428   11.1662001
     3   22.0810309   22.4907214   24.4131166
     4   18.4837535   18.5088507   18.0720244
     5   14.9082840   14.6820741   14.3899339
     6   16.4555825   16.5414748   17.5822953
```

Appendix G

Figures

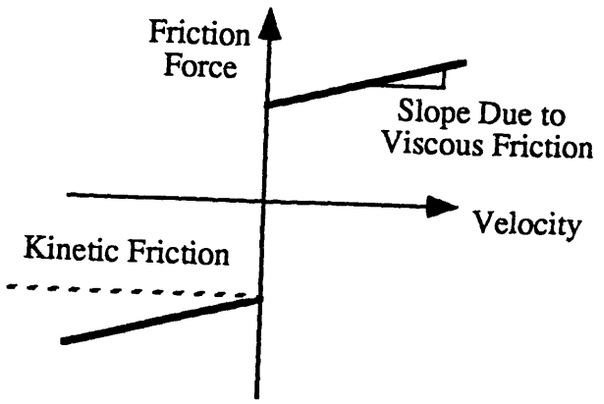

Figure G.1: Friction Model

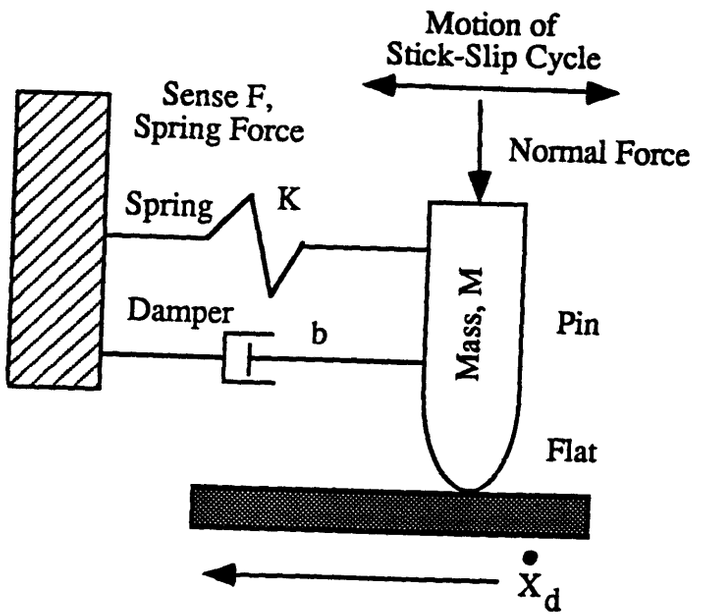

Figure G.2: Schematic of Rabinowicz Friction Model

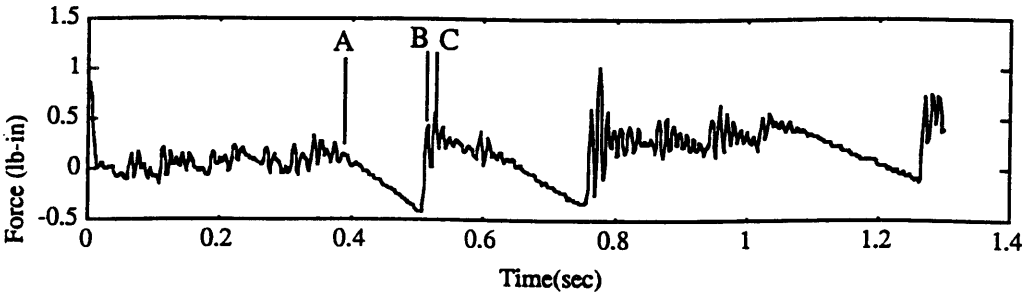

Figure G.3: Typical example of stick-slip force plot

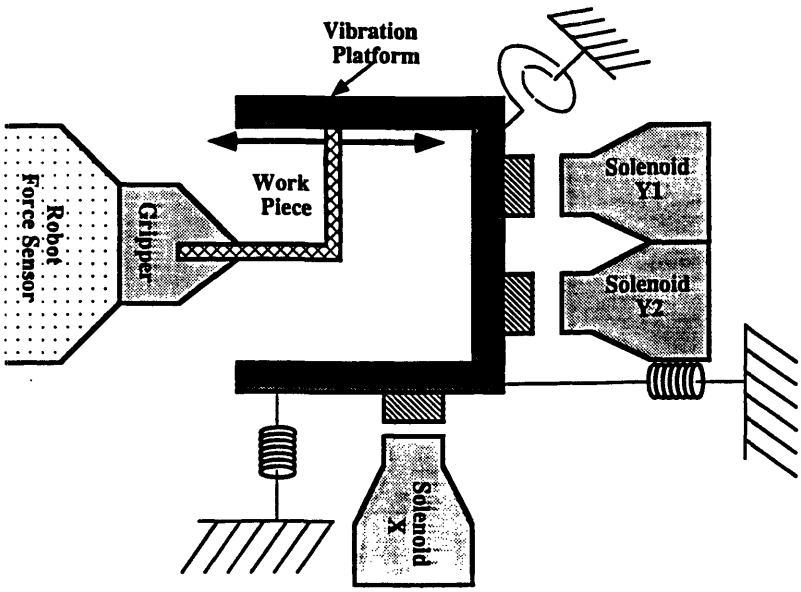

Figure G.4: The simplified schematic of the total working system

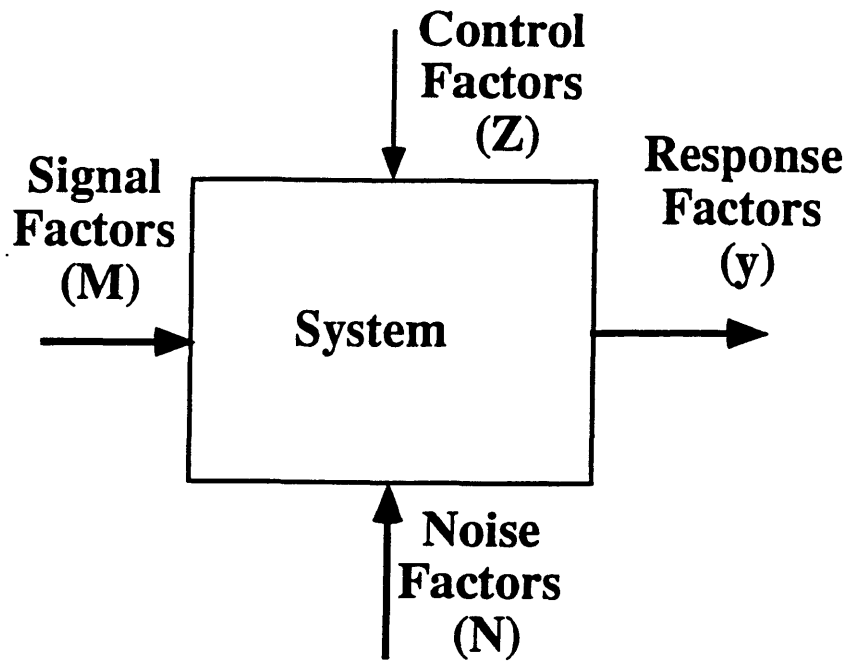

Figure G.5: Block diagram of a product/process

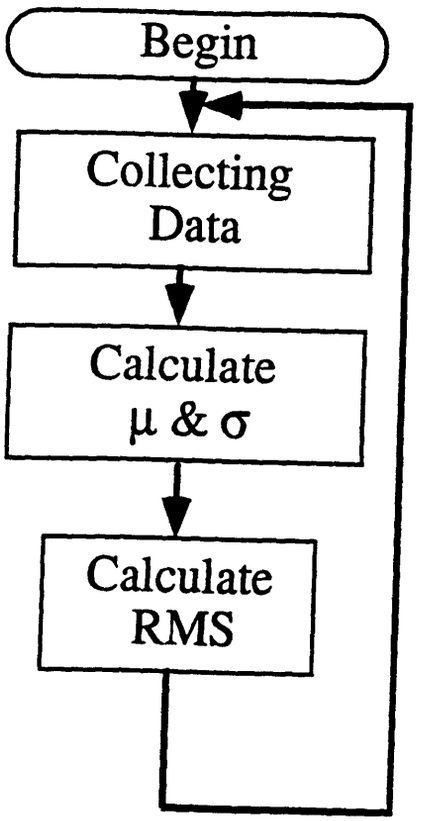

Figure G.6: Flowchart for the data acquisition

Exp	Xampv	Xfreq	Y1ampv	Y1freq	Y2ampv	Y2freq
1	5	8	5	8	5	8
2	5	8	5	8	5	8
3	5	8	5	8	10	16
4	5	8	5	8	10	16
5	5	8	10	16	5	8
6	5	8	10	16	5	8
7	5	8	10	16	10	16
8	5	16	10	16	10	16
9	5	16	5	16	5	16
10	5	16	5	16	5	16
11	5	16	5	16	10	8
12	5	16	5	16	10	8
13	5	16	10	8	5	16
14	5	16	10	8	5	16
15	5	16	10	8	10	8
16	5	8	10	8	10	8
17	10	8	5	16	5	16
18	10	8	5	16	5	16
19	10	8	5	16	10	8
20	10	8	5	16	10	8
21	10	8	10	8	5	16
22	10	8	10	8	5	16
23	10	8	10	8	10	8
24	10	16	10	8	10	8
25	10	16	5	8	5	8
26	10	16	5	8	5	8
27	10	16	5	8	10	16
28	10	16	5	8	10	16
29	10	16	10	16	5	8
30	10	16	10	16	5	8
31	10	16	10	16	10	16
32	10	16	10	16	10	16

Figure G.7: L32 orthogonal array

	Level 1	Level 2
Xamp V	5	10
Xfre Hz	8	16
Y1amp V	5	10
Y1fre Hz	8	16
Y2amp V	5	10
Y2fre Hz	8	16

Figure G.8: Input setting for the L32

Expt	X amp V	X fre Hz	Y1 amp V	Y1 Fre Hz	Y2 amp V	Y2 fre Hz
1	4	5	5	5	5	5
2	4	5	7.5	8	7.5	8
3	4	5	10	12	10	12
4	4	8	5	8	10	12
5	4	8	7.5	12	5	5
6	4	8	10	5	7.5	8
7	4	12	5	12	7.5	8
8	4	12	7.5	5	10	12
9	4	12	10	8	5	5
10	5	5	5	8	5	8
11	5	5	7.5	12	7.5	12
12	5	5	10	5	10	5
13	5	8	5	12	10	5
14	5	8	7.5	5	5	8
15	5	8	10	8	7.5	12
16	5	12	5	5	7.5	12
17	5	12	7.5	8	10	5
18	5	12	10	12	5	8
19	6	5	5	12	5	12
20	6	5	7.5	5	7.5	5
21	6	5	10	8	10	8
22	6	8	5	5	10	8
23	6	8	7.5	8	5	12
24	6	8	10	12	7.5	5
25	6	12	5	8	7.5	5
26	6	12	7.5	12	10	8
27	6	12	10	5	5	12

Figure G.9: Orthogonal array used for the experiment

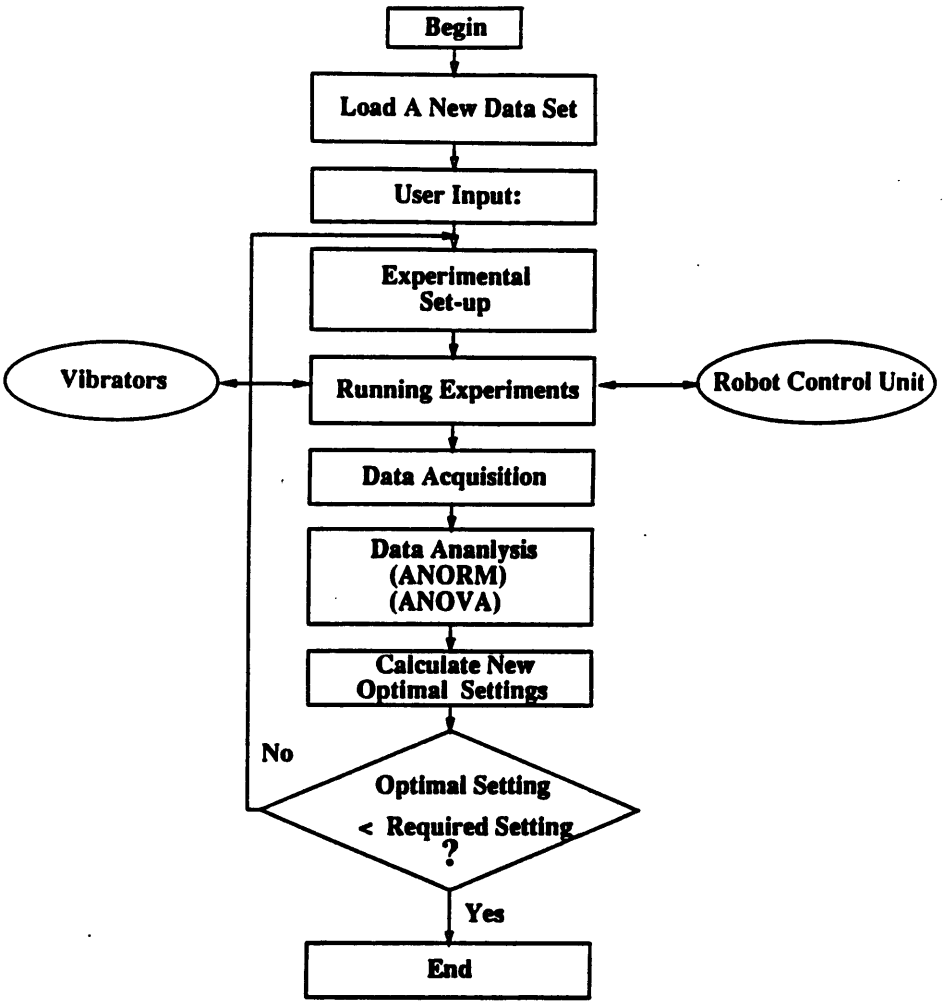

Figure G.10: Flowchart to automating the Taguchi Method

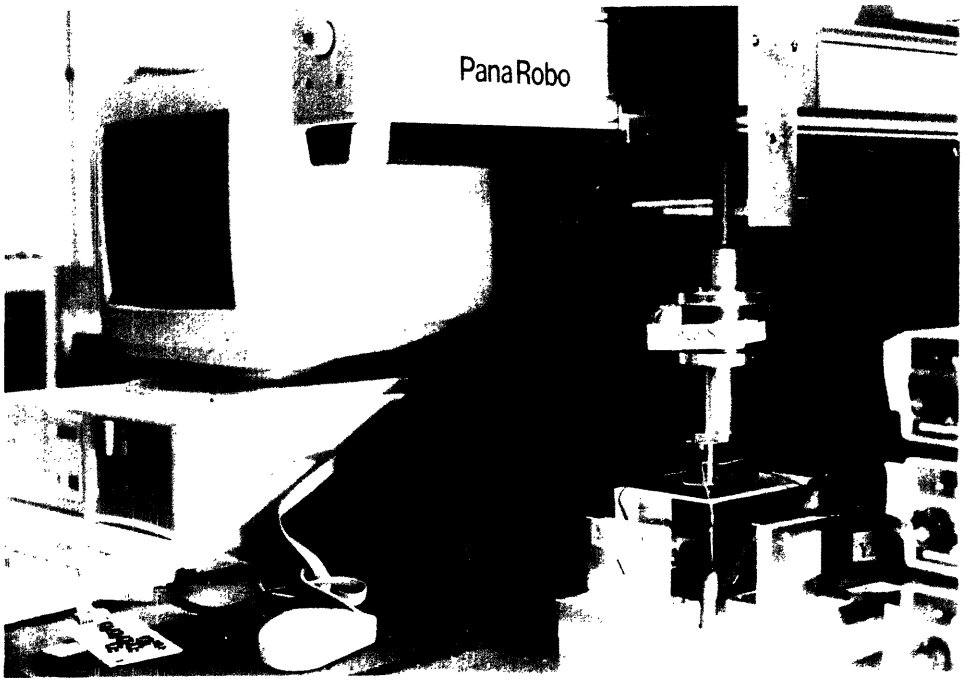

Figure G.11: Cable connector experiment set-up

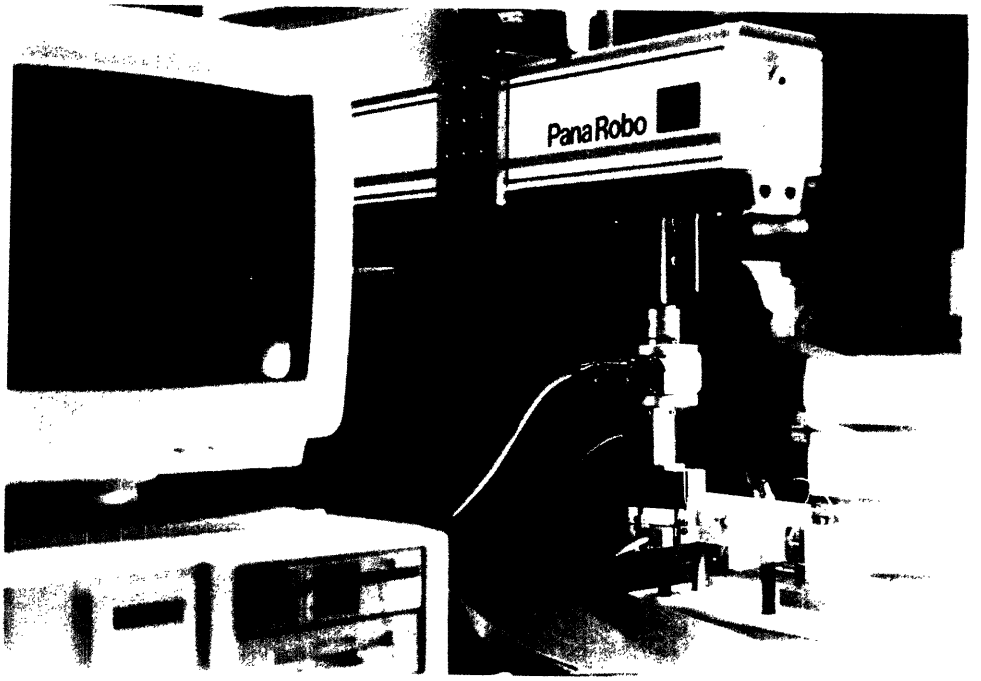

Figure G.12: Robot used for the experiments

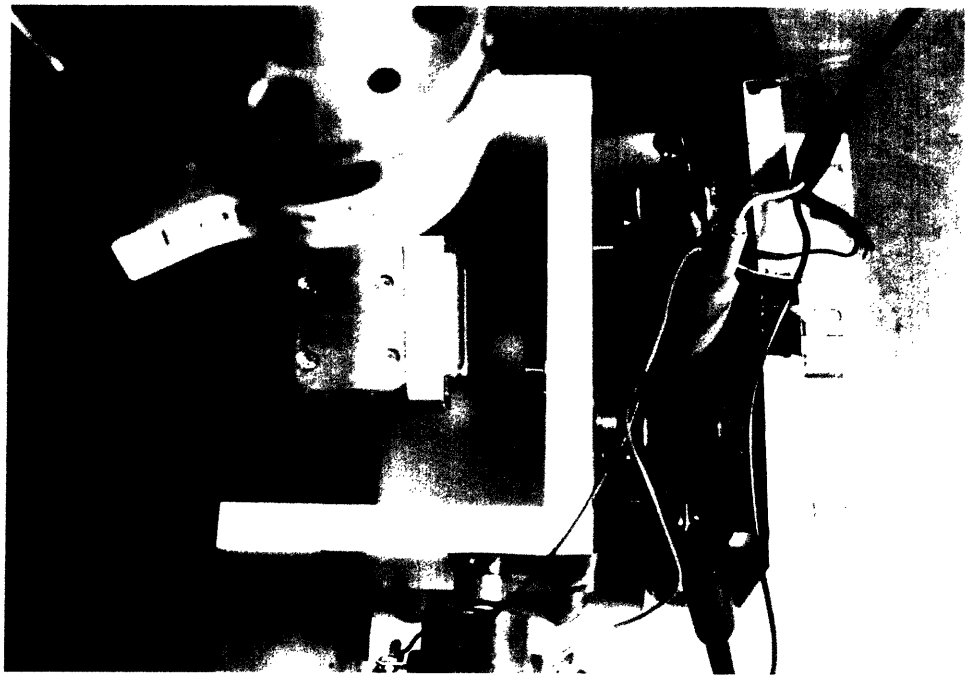

Figure G.13: Connectors used in the experiments

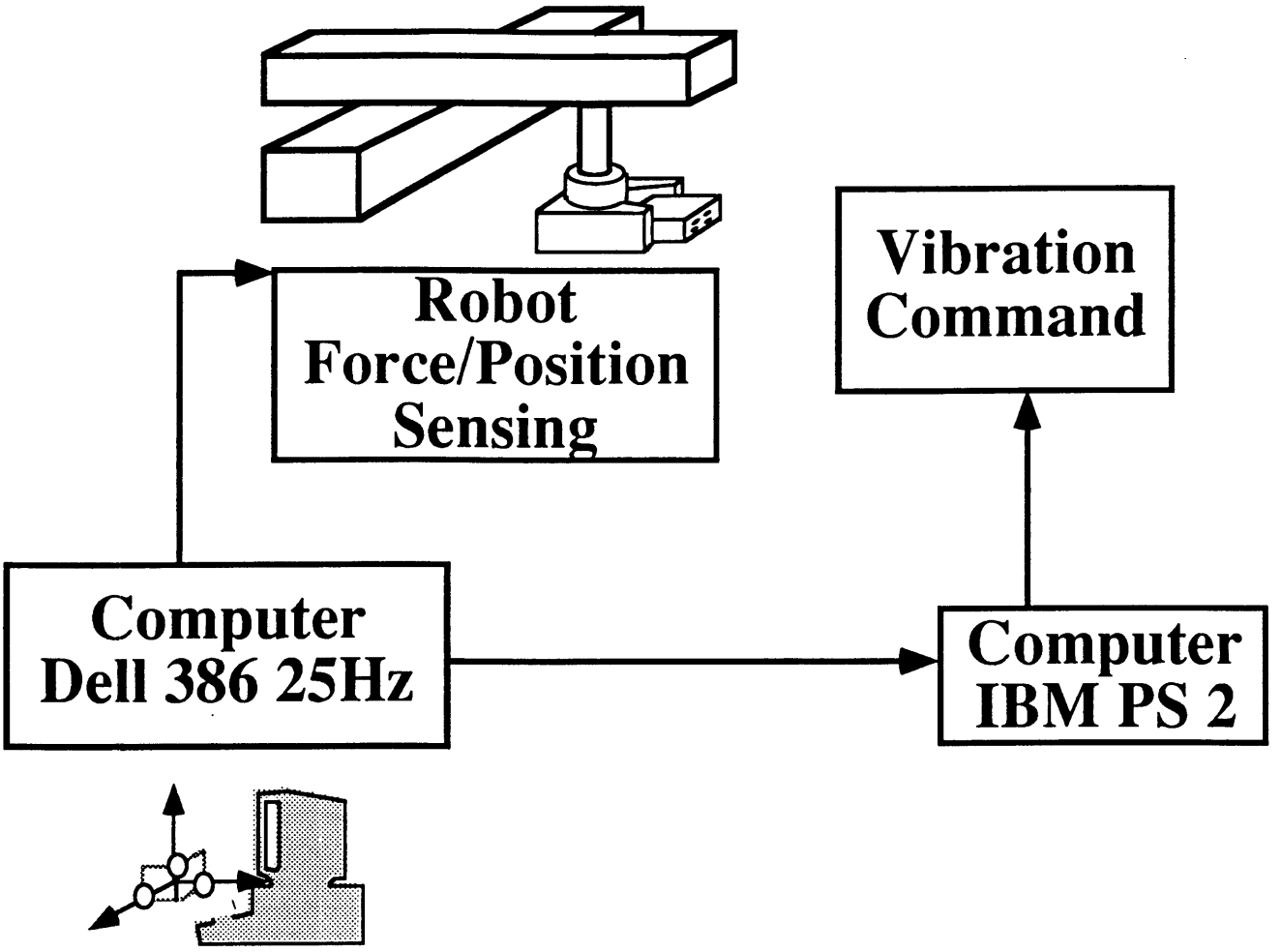

Figure G.14: Data acquisition diagram

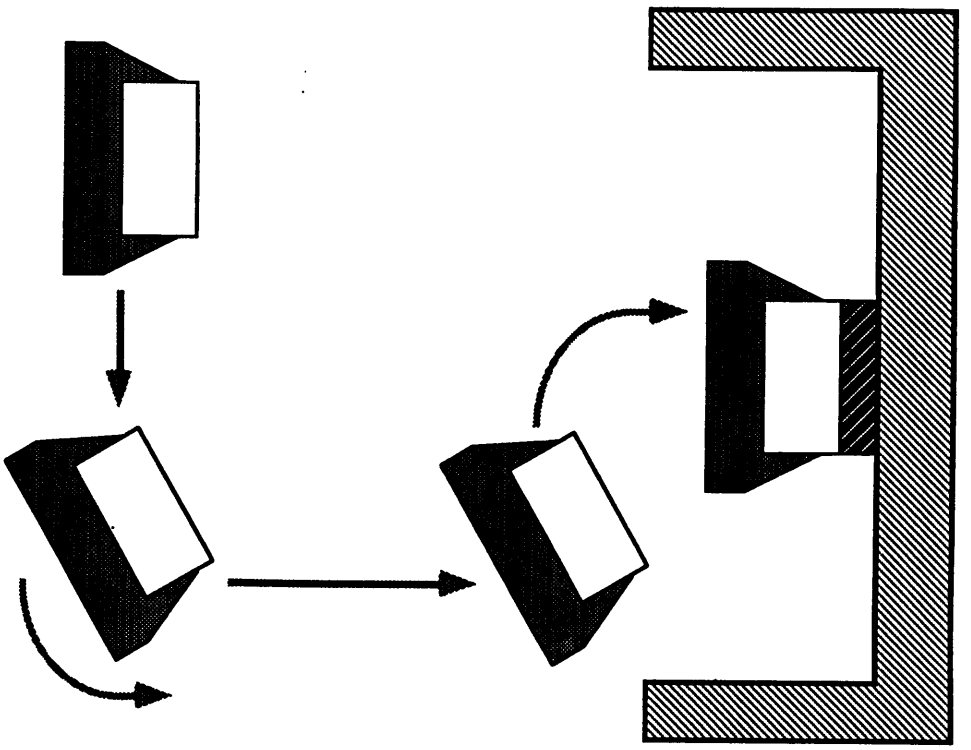

Figure G.15: The robot assembly trajectory

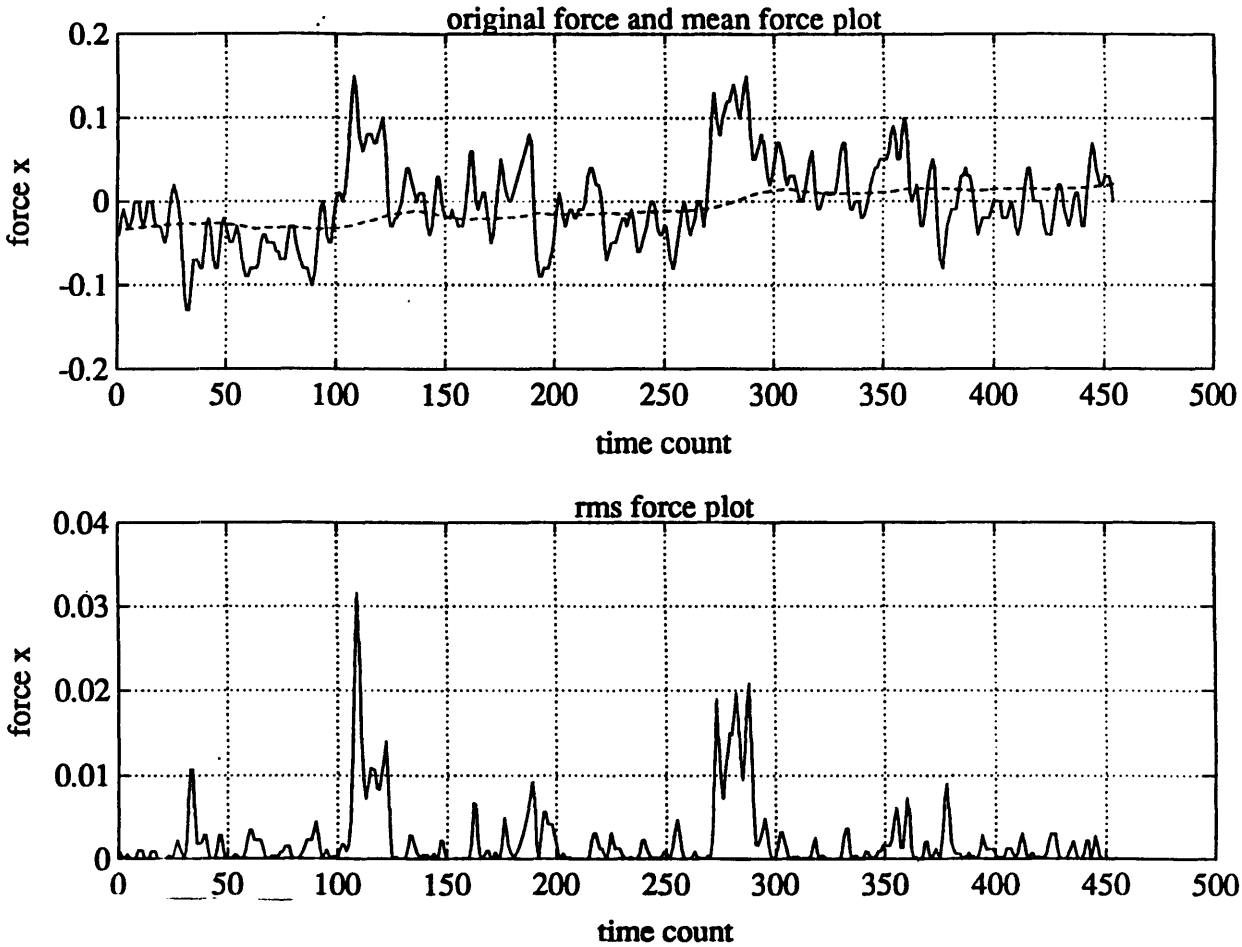

Figure G.16: A plot of a typical force trajectory together with its original data

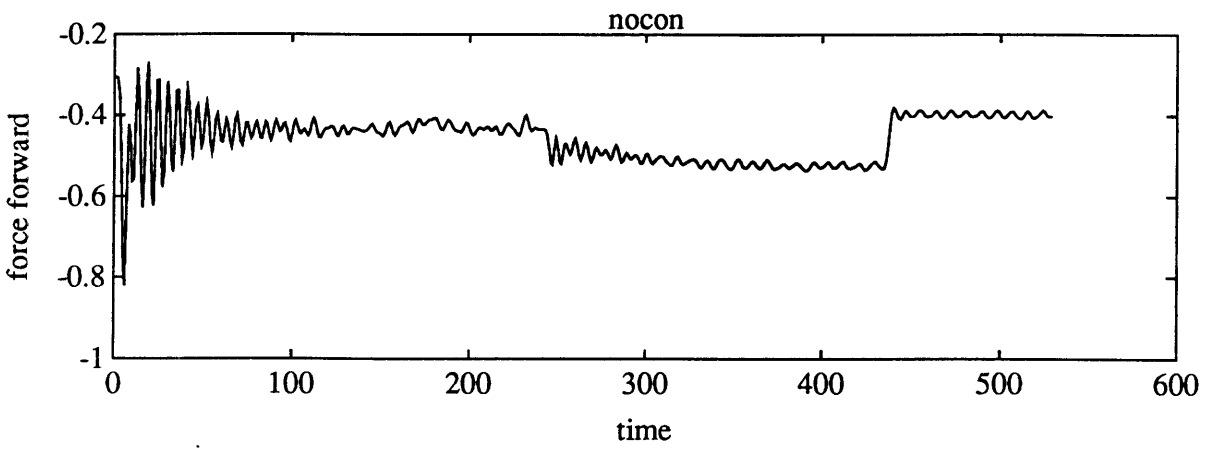

Figure G.17: Force and position plots for non-contact robot motion

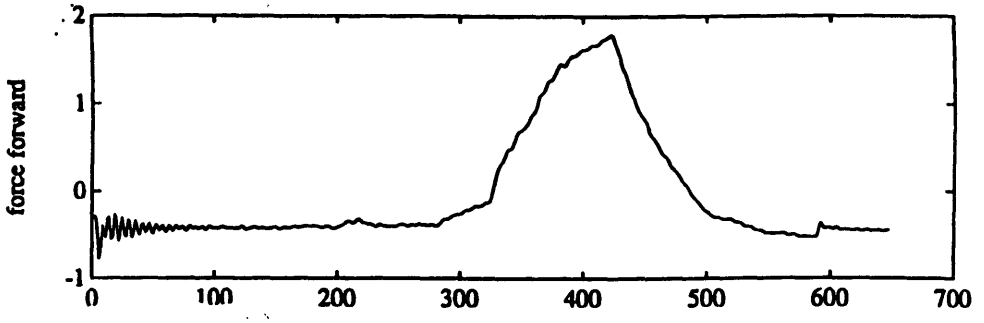

Figure G.18: Force and position plots for non-vibratory robot motion

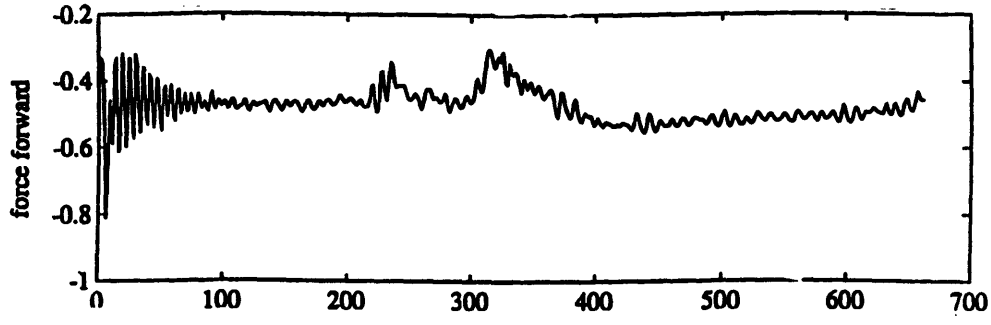

Figure G.19: Force and position plots for robot motion in optimal settings

Bibliography

Bibliography

[Asada 1990] Haruhiko Asada, "Teaching and Learning of Compliance using neural nets: Representation and Generation of Nonlinear Compliance", *IEEE International Conference on Robotics and Automation*, Cincinnati, Ohio, May 13-18, 1990

[Asada and Asari, 1988] H. Asada and Y. Asari, "The direct Teaching of Tool Manipulation Skills Via the Impedance Identification of Human Motions," *Proc. 1988 IEEE Inc. Conf. on Robotics and Automation*, pp. 1269 - 1274, 1988.

[Asada and Hirai, 1990] H. Asada and S. Hirai, "Toward a Symbolic-Level Feedback: Recognition of Assembly Process States," *Proc. 5-th Int. Symp. Robotics Res.*, Tokyo, 1990

[Asada and Hirai, 1990] S Hirai and H. Asada, "A Model-Based Approach to the Recognition of Assembly Process States for Symbolic-Level Feedback," *Proc. 1990 IEEE Int. Conf. on Robotics and Automation*, 1990.

[Asada and Kakumoto, 1991] H. Asada and Y. Kakumoto, "The Dynamics Analysis and Design of a High-Speed Insertion Hand Using the Generalized Centroid and Virtual Mass," *Trans. of ASME Vol 112*, Dec 1990.

[Asada and Liu 1991] Haruhiko Asada and Sheng Liu, " A Skill-based Adaptive Controller for Deburring Robots", *ASME Winter Annual Meeting*, Dec, 1991.

[Bowden and Leben 1939] Bowden, F.P. and Leben, L. 1939, "The nature of Sliding and the Analysis of Friction," *Proc. of the Royal Society, Series A,* vol, 169, p. 391- 431

[Dupuis 1992] Dupuis, Erick 1992, "Transfer of Assembly Skills from Humans to Robots", *S. M. Thesis. Massachusetts Institute of Technology. Dept. of Mechanical Engineering*, Jan., 1992

[Dokos 1943] Dokos, S.J. 1946, "Sliding Friction Under Extreme Pressure-1," *J. of Applied Mechanics*, vol. 13, series A, p.148- 56

[Li, 1991] Shih-Hung Li, "Implementation of Logical Branching Method with Three Approaches: Force Tolerance, Force Difference, and Confidence Method," *CIDMS 1991 Summer Mini-Conference*, July, 1991

[Lozano-Perez et al., 1984] Lozano-Perez, T., Mason, M. T., and Taylor, R. H., "Automatic Synthesis of Fine Motion Strategies for

Robotics," *Int. J Robotics Res.. Vol. 3, No.1*, pp. 3-24, 1984.

[Mason, 1982] Mason, M. T., "Compliant Motion," Brady, M. et al. eds., *Robot Motion*, Cambridge, MIT press, pp. 305-322, 1982.

[McCarragher and Asada 1991] B. McCarragher, H. Asada "The Recognition of Process State Transitions Using Dynamics Models for Robotic Assembly," submitted *ASME Winter Annual Conference 1991*, 1991

[Paul, Xu, Yun, 1991] Richard P. Paul, Yangsheng Xu, and Xiaoping Yun,"The Implementation of Hybrid Control in the Presence of Passive Compliance," *Robotic Research 5th International Symposium*, MIT Press, Cambridge, MA., 1990.

[Phadke, 1989] Phadke, Madhav S., *Quality Engineering Using Robust Design*, A T & T Bell Laboratories, Prentice-Hall 1989, p 6

[Rabinowicz 1951] Rabinowicz, E. 1951, "The Nature of the Static and Kinetic Coefficient of Friction," *J. of Applied Physics*, 22(11):1373-9

[Sampson *et al.* 1943] Sampson, J.B., Morgan, F., Reed, D.W. and Muskat, M. 1943, "Friction Behavior During the Slip Portion of the Stick-Slip Process," *J. of Applied Physics*, 14(12):689-700

[Simunovic, 1979] Simunovic, S. N., *An Information Approach to Parts Mating*, Ph.D. Thesis, Department of Electrical Engineering, Massachusetts Institute of Technology, 1979.

[Thomas 1930] Thomas, S. 1930, "Vibration Damped by Solid Friction," *Philosophical Magazine*, 7(9):329

[Whitney, 1982] Whitney, D. E., "Quasi-static assembly of compliantly supported rigid parts," *Int. J. Dynamic Systems, of Control, Measurement, Control 104*, March, pp. 65-77, 1982.